

1 **Cenozoic deformation in the Otway Basin, southern Australian margin: implications for**
2 **the origin and nature of post-breakup compression at rifted margins**

3 Simon P. Holford^{*}, Adrian K. Tuitt^{*}, Richard R. Hillis[†], Paul F. Green[‡], Martyn S. Stoker[§],
4 Ian R. Duddy[‡], Mike Sandiford[¶] & David R. Tassone^{*}

5 ^{*}Australian School of Petroleum, University of Adelaide, SA 5005, Australia

6 [†]Deep Exploration Technologies Cooperative Research Centre, 26 Butler Boulevard, Burbridge Business Park,
7 Adelaide Airport, SA 5950, Australia

8 [‡]Geotrack International Pty Ltd, 37 Melville Road, Brunswick West, VIC 5055, Australia

9 [§]British Geological Survey, Murchison House, West Mains Road, Edinburgh EH9 3LA, UK

10 [¶]School of Earth Sciences, University of Melbourne, VIC 3010, Australia

11 Corresponding author: simon.holford@adelaide.edu.au

12
13 **ABSTRACT**

14 There is growing recognition that pulses of compressive tectonic structuring punctuate the
15 post-breakup subsidence histories of many ‘passive’ rifted continental margins. In order to
16 obtain new insights into the nature and origin of compression at passive margins we have
17 conducted a comprehensive analysis of the post-breakup (<43 Ma) deformation history of the
18 offshore Otway Basin, southern Australian margin, using a regional seismic database tied to
19 multiple wells. Through mapping of a number of regional intra-Cenozoic unconformities we
20 have determined growth chronologies for a number of major anticlinal structures, most of
21 which are ~NE-SW-trending folds that developed during mild inversion of syn-rift normal
22 faults or through buckling of the post-rift succession. These chronologies are supplemented
23 by onshore structural evidence and by thermochronological data from key wells. Whilst our
24 analysis confirms the occurrence of a well-documented pulse of late Miocene–early Pliocene
25 compression, post-breakup deformation is not restricted to this time interval. We highlight the
26 growth of a number of structures during the mid-late Eocene and the Oligocene-early

27 Miocene, with evidence for considerable temporal and spatial migration of strain within the
28 basin. Our results indicate a long-lived ~NW-SE maximum horizontal stress orientation since
29 the mid-late Eocene, consistent with contemporary stress observations but at variance with
30 previous suggestions that this stress orientation was initiated in the late Miocene by increased
31 coupling of the Australian-Pacific plate boundary. We attribute the observed record of
32 deformation to a compressional intraplate stress field, coupled to the progressive evolution of
33 the boundaries of the Indo-Australian Plate, ensuring that this margin has been subject to
34 ongoing compressional forcing since mid-Eocene breakup. Our results indicate that
35 compressional deformation at passive margins may be more common than is generally
36 assumed, and that passive margin basins with evidence for protracted post-breakup
37 deformation histories can provide useful natural laboratories for obtaining improved
38 understanding of the evolution of intraplate stress fields over geological timescales.

39

40 INTRODUCTION

41 In recent years, seismic exploration of rifted continental margins has provided growing
42 evidence that the post-rift evolution of some margins is not characterized solely by tectonic
43 quiescence and dominantly extensional stress regimes, as implicit in many models of
44 ‘passive’ margin evolution (Bond & Kominz, 1988). In fact, the post-rift subsidence histories
45 of many passive continental margins worldwide have been punctuated by pulses of localised
46 compressional shortening (i.e. tectonic inversion; Williams *et al.* 1989; Turner & Williams,
47 2004) that are often accompanied by regional uplift, producing long-wavelength (>200-500
48 km) low-angle ($\leq 5^\circ$) unconformities (Doré *et al.*, 2002; Praeg *et al.*, 2005; Johnson *et al.*,
49 2008). Margins that provide evidence for post-rift compression include: the NW European
50 Atlantic margin (Boldreel & Anderson, 1998; Vågnes *et al.*, 1998; Lundin & Doré, 2002;
51 Davies *et al.*, 2004; Stoker *et al.*, 2005; Williams *et al.*, 2005; Doré *et al.*, 2008; Hillis *et al.*,

52 2008a; Holford *et al.*, 2008, 2010a; Tuitt *et al.*, 2010); the Iberian margin (Peron-Pinvidic *et al.*, 2008; Vasquez *et al.*, 2008; Pereira *et al.*, 2011); the eastern US margin (Kulpecz *et al.*, 2009); the NE Brazilian margin (Cobbold *et al.*, 2001, 2007, 2010); the western African (Angolan) margin (Hudec & Jackson, 2002); and the Australian NW Shelf (Harrowfield & Keep, 2005; Hillis *et al.*, 2008b). Constraining the timing, distribution and ultimately the origin of post-rift compression has important economic implications, as compressional folding of syn-rift and post-rift sedimentary successions can produce significant hydrocarbon traps (e.g. the Ormen Lange Dome on the mid-Norwegian margin; Vågnes *et al.*, 1998). Moreover, the near-continuous history of post-rift sedimentary deposition at many margins provides them with the potential capability of serving as sensitive recorders of geodynamic events and processes. Careful examination of the timing and distribution of post-breakup compressional structures and unconformities at passive margins may thus yield important insights to generic problems like the evolution of intraplate stress fields (Zoback & Zoback, 2007) or the impact of mantle flow on surface topography (Braun, 2010).

66

67 This paper examines the record of post-breakup compression in the offshore Otway Basin of the southern Australian margin. The Otway Basin is one of several depocentres that formed during Cretaceous-Palaeogene continental breakup between Antarctica and Australia (Norvick & Smith, 2001). Along this margin, compressional structures have been most commonly identified within the post-rift Cenozoic successions of the Otway, Gippsland and Bass basins (Hill *et al.*, 1995; Perineck & Cockshell, 1995; Dickinson *et al.*, 2001; Hillis *et al.*, 2008b), and many significant producing oil and gas fields in these basins are hosted within Cenozoic anticlines (Bernecker *et al.*, 2003; Holford *et al.*, 2011a). Similar Cenozoic anticlines occur within the Torquay sub-basin (Holford *et al.*, 2011b) but drilling has shown that they do not contain significant quantities of hydrocarbons (Trupp *et al.*, 1994), implying

77 that the relative timing of compressional deformation with respect to hydrocarbon generation
78 and charge is a key factor in defining prospectivity along the margin (Duddy, 1997; Holford
79 *et al.*, 2010b).

80

81 Previous studies in the Otway Basin have identified major periods of compressional
82 deformation and resultant fold growth during the mid-Eocene (Duddy *et al.*, 2003) and late
83 Miocene-Pliocene (Dickinson *et al.*, 2001, 2002). It is generally accepted that Cenozoic
84 deformation of the southern Australian margin (which continues to the present-day as
85 evidenced by elevated levels of intraplate seismicity and seismogenic strain rates of up to
86 $\sim 10^{16} \text{ s}^{-1}$ (C  lerier *et al.*, 2005; Sandiford & Egholm, 2008; Holford *et al.*, 2011c) is
87 controlled to first-order by plate boundary forces (Fig. 1) (Sandiford *et al.*, 2004; Hillis *et al.*,
88 2008b; M  ller *et al.*, 2012). As is common with many studies of post-rift compression at
89 passive margins (e.g. Holford *et al.*, 2009a), previous investigations in the Otway Basin have
90 often sought to identify a sole driving mechanism responsible for the major pulses of
91 deformation, usually a far field, plate boundary tectonic event. For example, late Miocene-
92 Pliocene fault reactivation and faulting in the Otway Basin has been variously ascribed to the
93 contemporaneous collision of Australia's northern margin with the island arc in New Guinea
94 (Hill *et al.*, 1995), or increased coupling of the Australian-Pacific plate boundary resulting
95 from formation of the Southern Alps in New Zealand (Fig. 1) (Dickinson *et al.*, 2002). Whilst
96 such events undoubtedly exert a significant control on the coeval intraplate stress field
97 (Sandiford *et al.*, 2004), recent investigations of the timing of Cenozoic post-breakup
98 deformation along the NW European Atlantic margin have described multiple structures with
99 evidence for growth at various times subsequent to early-Eocene breakup, indicating that
100 post-breakup deformation is more common than generally assumed and not necessarily

101 restricted to discrete temporal pulses (Vagnes *et al.*, 1998; Doré *et al.*, 2008; Ritchie *et al.*,
102 2008; Holford *et al.*, 2009a).

103

104 Here we present the first comprehensive analysis of the timing of Cenozoic post-breakup
105 (<43 Ma) shortening in the Otway Basin of the southern Australian margin, using a regional
106 2D seismic database calibrated to biostratigraphic data from exploration wells (Fig. 2). We
107 have identified a number of major offshore compressional structures and where possible have
108 correlated them with contiguous terrestrial structures identified by onshore mapping studies.
109 Our analysis indicates that the growth of these structures, and thus the chronology of post-
110 breakup compressional deformation in the Otway Basin, is not restricted to a narrow time
111 interval, and there appears to have been substantial spatial and temporal migration of strain
112 within the basin. Individual structures display a variety of ages from mid-Eocene to early
113 Pliocene, although several periods of enhanced deformation (mid-Eocene and late Miocene)
114 are apparent. Although some peaks in tectonic activity coincide with far-field events at plate
115 boundaries, such as collisional events in New Guinea and New Zealand, we suggest that no
116 single event is responsible for the record of deformation described herein. Instead, we
117 propose that post-breakup deformation in the Otway Basin reflects an evolving
118 compressional intraplate stress field controlled by progressive reconfigurations of the Indo-
119 Australian plate boundaries over the past ~43 Myr, with key episodes of enhanced
120 deformation corresponding to major reorganisations of the Indo-Australian Plate boundaries.

121

122 **TECTONIC SETTING OF THE OTWAY BASIN**

123 The Otway Basin is a large, broadly NW-SE trending extensional basin (maximum total
124 sediment thickness ~13 km) encompassing onshore and offshore parts of South Australia
125 (SA) and Victoria, and Tasmanian waters (Fig. 2). The basin developed following late

126 Jurassic-early Palaeogene rifting, breakup and eventual separation of Australia and Antarctica
127 (Krassay *et al.*, 2004). Exploration of the basin is at a mature stage with over 200 wells
128 drilled in the basin, resulting in several commercial gas discoveries offshore Victoria and
129 numerous smaller onshore gas and CO₂ fields. To date, there have been no commercial oil
130 discoveries. Most offshore exploration has been in relatively shallow water depths (<250 m),
131 but is progressively focused on deep-water plays. Amrit-1 was drilled in 1,425 m of water in
132 2004, representing the deepest well drilled along the southern Australian margin yet, and
133 acreage in the western Otway Basin released in 2012 reaches water depths of 3000 m
134 (Totterdell, 2012).

135

136 A number of variably exposed tectonostratigraphic basement provinces underlie the Otway
137 Basin (Fig. 2d). Much of the South Australian and western Victorian basin is underlain by
138 terranes that form part of the Cambrian-Ordovician Delamerian fold belt (e.g. the
139 Kanmantoo-Glenelg Zone and Grampians-Stavely Zone) or the mid-Palaeozoic Lachlan fold
140 belt (e.g. the Stalwell Zone and Bendigo Zone) (Cayley *et al.*, 2002; Gibson *et al.*, 2011). The
141 boundaries between these terranes strike broadly ~N to NNW. These terranes are separated
142 from the Neoproterozoic to Cambrian Selwyn-Taswegia Block, which underlies most of the
143 Torway sub-basin and Tasmania by a major ~N-S striking boundary named the Avoca Fault
144 (Gibson *et al.*, 2011). The Avoca Fault is interpreted to continue offshore as the Sorell Fault,
145 a major reactivated basement structure that accommodated significant transform motion
146 during the separation of Australia and Antarctica, which may continue into the Southern
147 Ocean as the Tasman Fracture Zone (Gibson *et al.*, 2011, 2013). An abrupt change in the
148 orientation of Cretaceous normal faults, from ~NW-SE to the west of the Avoca Fault to
149 ~NE-SW to the east points to an important basement control on later rifting episodes (Miller
150 *et al.*, 2002).

151 Rifting in the Otway Basin commenced in the late Jurassic-early Cretaceous (Fig. 3) first in
152 the west then progressing to the east, resulting in several distinct grabens and half-grabens
153 with varying geometries and orientations (Fig. 2) (Perineck & Cockshell, 1995; Krassay *et*
154 *al.*, 2004). The early Cretaceous rift axis is located onshore and consists of ~W to NW
155 trending depocentres in the west (e.g. the Robe and Penola Troughs in SA) and ~NE trending
156 depocentres in the east (e.g. Torquay sub-basin in Victoria), with the variation in trends
157 largely reflecting the basement heterogeneities described above (Miller *et al.*, 2002; Krassay
158 *et al.*, 2004). Initial rift fills were dominated by carbonaceous lacustrine shales with minor
159 interbedded sandstones and volcanics (Casterton Formation), and as the rate of extension
160 increased into the Berriasian and Barremian syn-rift accommodation space was filled by
161 amalgamated fluvial and lacustrine facies (Crayfish Subgroup) (Krassay *et al.*, 2004). A thick
162 mudstone-rich volcanoclastic succession (Eumeralla Formation) was deposited during a
163 decrease in tectonic activity during the Aptian and Albian (Krassay *et al.*, 2004). The main
164 source rocks in the Otway Basin are of early Cretaceous age (Casterton Formation and
165 Crayfish Subgroup in SA and Eumeralla Formation in Victoria), and the Pretty Hill
166 Formation (Crayfish Subgroup) is the major reservoir unit in the SA Otway Basin (Bernecker
167 *et al.*, 2003).

168

169 This basin and other parts of the southern Australian margin experienced a pulse of ~NW-SE
170 directed shortening, uplift and exhumation during the late Albian-Cenomanian (Duddy, 1997,
171 2003; Hill *et al.*, 1995; MacDonald *et al.*, 2013), resulting in a regional mid-Cretaceous
172 unconformity (MCU) (Fig. 3, 4). Major uplift in the eastern Otway Basin in the present-day
173 Otway Ranges effectively isolated the Torquay sub-basin (Krassay *et al.*, 2004), whose late
174 Cretaceous-Cenozoic stratigraphy shares a closer affinity with the Bass Basin to the east
175 (Messent *et al.*, 1999). Western and central parts of the Otway Basin experienced renewed

176 ~N-S to ~NE-SW directed rifting in the late Cretaceous (Perineck *et al.*, 1994), with some
177 workers arguing for a significant oblique (sinistral) component (Schneider *et al.*, 2004). The
178 locus of extension shifted to the south during the late Cretaceous, resulting in a series of
179 ~NW-SE depocentres (the Morum and Nelson sub-basins) located to the south of the
180 Tartwaup-Mussel fault zone (Bernecker *et al.*, 2003). Oblique-slip reactivation of N-S
181 basement trends during ~NE-SW extension resulted in a series of ~N-S axial anticlinal and
182 synclinal folds with a wavelength of ~5-15 km (Geary & Reid, 1998). The Upper Cretaceous
183 Sherbrook Group generally comprises fluvial-deltaic and nearshore to shallow-marine
184 siliclastic deposits, with the basal Waarre Formation acting as the major regional reservoir
185 interval in the Victorian part of the Otway Basin.

186

187 Despite much research, the history of rifting and breakup between Australia and Antarctica
188 remains poorly constrained (e.g. Williams *et al.*, 2011; Gibson *et al.*, 2013). It is generally
189 agreed rifting in the Otway Basin culminated at the end of the Cretaceous and is marked by a
190 regional intra-Maastrichtian unconformity (IMU), which is interpreted by some as marking
191 the time of continental plate separation between Australia and Antarctica (Krassay *et al.*,
192 2004). However, there is no evidence for appreciable seafloor spreading off the Otway Basin
193 at this time, with first ocean crust in the Otway Basin dated as middle Eocene (Norvick &
194 Smith, 2001). Sedimentary successions in the Otway Basin become progressively more
195 marine-influenced and calcareous throughout the Cenozoic, reflecting the progressive
196 establishment of open marine circulation (McGowran *et al.*, 2004; Blevin & Cathro, 2008).
197 Subsidence following the development of the intra-Maastrichtian unconformity initiated a
198 major transgression across the Otway Basin resulting in deposition of the siliclastic
199 Wangerrip Group (Bernecker *et al.*, 2003). Small growth wedges bounded by basinward-
200 dipping reactivated late Cretaceous normal faults in the Portland Trough, onshore and

201 offshore Victoria (Krassay *et al.*, 2004) imply that an extensional stress regime continued into
202 the Palaeogene. The Wangerrip Group reaches a maximum thickness of >1200 m within the
203 Portland Trough (Holdgate & Gallagher, 2003). It is separated by a major intra-Lutetian
204 unconformity (ILU) associated with significant localised erosion from the overlying
205 prograding nearshore to offshore marine clastics and carbonates of the late Eocene-early
206 Oligocene Nirranda Group (Holdgate & Gallagher, 2003; Krassay *et al.*, 2004). This
207 unconformity correlates with the onset of fast seafloor spreading in the southern Ocean at ~43
208 Ma (Veevers, 2000; McGowran *et al.*, 2004), and is associated with localised magmatic
209 activity in both the Ceduna (Jackson, 2012) and Otway basins (Holford *et al.*, 2012). The
210 Nirranda Group reaches its maximum thickness of ~200 m in two major depocentres, in the
211 Port Campbell Embayment and Portland Trough (Holdgate & Gallagher, 2003). It is
212 separated from the overlying Heytesbury Group by a regional intra-Oligocene unconformity
213 (IOU) (Bernecker *et al.*, 2003). The late Oligocene-late Miocene Heytesbury Group
214 (maximum thickness >1600 m) comprises marls and limestones deposited under fully marine
215 conditions (Krassay *et al.*, 2004). A regional, late Miocene-Pliocene unconformity (MPU)
216 (Dickinson *et al.*, 2002; Holford *et al.*, 2011b) separates the Heytesbury Group from the late
217 Neogene succession of the Otway Basin which is characterised by relatively thin and
218 localised mixed siliclastic-carbonate sediments and basaltic volcanic rocks that usually
219 unconformably or disconformably overlie Heytesbury Group strata (Dickinson *et al.*, 2002;
220 Tassone *et al.*, 2011).

221

222 Since the mid-Eocene onset of fast spreading ~43 Myr ago (Veevers, 2000; McGowran *et al.*,
223 2004), the Australian continent has been subjected to a largely compressional stress field
224 resulting from the configuration of the Indo-Australian Plate boundaries (Fig. 1) (Sandiford
225 & Quigley, 2009). This compression has caused widespread tectonic inversion in the

226 sedimentary basins around and within the Australian continent (Etheridge *et al.*, 1991), and
227 has had a profound influence on hydrocarbon occurrence by creating or amplifying traps in
228 central Australia, the NW Shelf and the southern Australian margin (Hillis *et al.*, 2008b;
229 Holford *et al.*, 2010b). With respect to the southern margin, compressional deformation has
230 been documented most comprehensively in the Gippsland Basin, where several of Australia's
231 largest hydrocarbon fields are located in inversion-related anticlines that mostly trend ~NE-
232 SW or ~ENE-WSW (Hillis *et al.*, 2008b). Workers have identified key periods of deformation
233 during the Eocene, Oligocene-early Miocene, and late Miocene-Pliocene (Brown, 1986;
234 Dickinson *et al.*, 2001). A number of structures, including the anticline that hosts the
235 Barracouta gas field, reveal evidence for multiple phases of growth (in this case, Oligocene-
236 early Miocene and Plio-Pleistocene) (Dickinson *et al.*, 2001). From a seismic analysis of the
237 late Oligocene-Recent Seaspray Group, Dickinson *et al.* (2001) identified two main structural
238 styles that characterise Cenozoic compressional deformation in the Gippsland Basin: 1)
239 reactivation and inversion of basin-margin normal faults with associated high amplitude
240 hangingwall anticlines; and 2) broad low-relief anticlines in the main depocentre of the basin
241 reflecting reactivation of deep fault blocks.

242

243 In comparison to the Gippsland Basin, the timing and distribution of Cenozoic compressional
244 deformation in the Otway Basin is far less well understood. The most significant
245 compressional structures occur onshore in the eastern Otway Basin, in and around the Otway
246 Ranges, and in the adjacent Torquay sub-basin (Hill *et al.*, 1995; Dickinson *et al.*, 2002;
247 Sandiford *et al.*, 2004; Clark *et al.*, 2012; Tassone *et al.*, 2012, 2013). Similar to the
248 Gippsland Basin, these structures comprise a combination of ~NE-SW trending high and
249 low-amplitude anticlines resulting from reactivation of syn-rift normal faults. Most studies
250 have assigned a late Miocene-Pliocene age to the formation of these structures (Hill *et al.*,

1995; Dickinson *et al.*, 2002; Hillis *et al.*, 2008b) and other anticlines and reactivated faults identified elsewhere in the Otway Basin (Perineck & Cockshell, 1995; Schneider *et al.*, 2004). In contrast to the Gippsland Basin, relatively few instances of Eocene-Oligocene growth of compressional structures in the Otway Basin have been reported. Exceptions include the Morum High on the outer continental shelf in the western Otway Basin, which Duddy *et al.* (2003) recognized as a mid-Eocene inversion structure.

257

258 SEISMIC DATABASE AND METHODOLOGY

With a few exceptions (e.g. Perineck & Cockshell, 1995), the majority of previous studies of structural styles in the Otway Basin have focused on individual structures (e.g. Schneider *et al.* 2004) or specifically on the South Australian (Jensen-Schmidt *et al.*, 2002) or Victorian (Hill *et al.*, 1995) sectors of the basin. With the aim of developing a better understanding of the basin-wide distribution and chronology of post-breakup compression, we have conducted seismic-stratigraphic and structural interpretation and mapping of a regional 2D seismic dataset that covers the length and breadth of the offshore Otway Basin (Fig. 2). The seismic data comprises part of PGS's Southern Australian Margin Digital Atlas (SAMDA), a compilation of ~113,000 line-kilometres of 2D seismic data from 129 separate surveys provided by federal (Geoscience Australia) and state governments (Primary Industries and Resources South Australia, and Department of Primary Industries Victoria). Our mapping of compressional structures in the Otway Basin utilizes ~30,000 line-kilometres of 2D seismic data from 14 individual surveys, and is calibrated to stratigraphic information from 17 offshore wells (Fig. 3).

273

In order to define the timing of post-breakup compression in the offshore Otway Basin we have conducted detailed mapping of three critical stratigraphic horizons that bound the major

276 Cenozoic supersequences of the Otway Basin (Fig. 5). These horizons we have mapped are;
277 an intra-Maastrichtian (~67 Ma) unconformity (IMU) that occurs at the top of the Sherbrook
278 Group and base of the Wangerrip Group; an intra-Lutetian (~46-43 Ma) unconformity (ILU)
279 that occurs at the top of the Wangerrip Group and the base of the Nirranda Group; and, an
280 intra-Oligocene (~29-28 Ma) unconformity (IOU) that occurs at the top of the Nirranda
281 Group and the base of the Heytesbury Group (Fig. 3, 4; Boulton *et al.*, 2002; Holdgate &
282 Gallagher, 2003; Krassay *et al.*, 2004). Where possible, we have also mapped the distribution
283 of the late Miocene-Pliocene (~10-5 Ma) unconformity (MPU) that marks the top of the
284 Heytesbury Group (Dickinson *et al.*, 2002), though as this surface often occurs at shallow
285 depths (less than several hundred metres) where the quality of available seismic data is often
286 poor and biostratigraphic constraints are limited, it is not possible to confidently map the
287 unconformity throughout the basin. A regional sequence-stratigraphic study by Krassay *et al.*
288 (2004) which utilized biostratigraphic constraints from ~80 exploration wells showed that
289 these unconformities can be traced throughout the onshore and offshore Otway Basin. All
290 three unconformities are locally associated with severe erosion, and the intra-Maastrichtian
291 and intra-Lutetian unconformities are at least in part tectonically controlled (Krassay *et al.*,
292 2004; McGowran *et al.*, 2004). The age-ranges of these unconformities are generally well
293 constrained by planktonic foraminifera and palynological data from onshore and offshore
294 exploration wells (McGowran *et al.*, 2004). These unconformities are broadly coeval with
295 other unconformities and sequence boundaries of similar age that occur along almost the
296 entire length of the southern Australian margin, from the Ceduna Basin in the west to the
297 Gippsland Basin in the east (McGowran *et al.*, 2004; Blevin & Cathro, 2008).

298

299

300

301 POST-BREAKUP DEFORMATION STRUCTURES IN THE OTWAY BASIN

302 Here we describe results from mapping of seven anticlinal structures within the Cenozoic
303 succession of the Otway Basin that formed during post-breakup compressional deformation.
304 We applied conventional seismic-stratigraphic methodology (e.g. Mitchum *et al.*, 1977) for
305 identifying and interpreting reflection terminations to map the intra-Maastrichtian, intra-
306 Lutetian and intra-Oligocene unconformities. These dated horizons were then used to identify
307 features such as thickness variations across hinge zones and onlapping reflections towards
308 anticline limbs, to help constrain the age and chronology of individual structures related to
309 compressional deformation. The amplitudes of the anticlines range from ~100 to 500 m and
310 the lengths of their axial traces vary between ~4 and 30 km. Two dominant structural trends
311 are identified, ~NE-SW and ~NW-SE.

312

313 Morum Anticline

314 The Morum Anticline is located ~65 km SW of Cape Jaffa, South Australia (Fig. 2b). This
315 anticline is partially responsible for a structural culmination with significant bathymetric
316 expression located near the continental shelf break, known as the Morum High. Local
317 stratigraphic constraints are provided by the Morum-1 well, which intersected thin
318 unconformity-bound Heytesbury (~138 m) and Wangerrip Group (~68 m) sequences
319 overlying a thick Upper Cretaceous Sherbrook Group (~1656 m) succession (Duddy *et al.*,
320 2003). The well was drilled in 1975 and no significant shows were encountered.

321

322 The Morum Anticline trends ~NE-SW, has an axial trace ~19 km long and has a maximum
323 amplitude of ~100 m (Fig. 6). Figure 6 shows that Cretaceous and older sediments in the fold
324 are offset by a number of NW-trending normal faults, which form a series of fault blocks that
325 run obliquely to the axis of the fold. Palaeocene-early Eocene Wangerrip Group sediments

326 appear to thicken away from the crest of the fold and show no evidence for onlap onto the
327 IMU. The top-Wangerrip Group unconformity (ILU) is an angular unconformity that
328 separates tilted Wangerrip Group strata from relatively horizontal reflections in the overlying
329 Heytesbury Group. A ~NNE-SSW-oriented seismic profile through the Morum Anticline
330 shows clear truncations within the Wangerrip Group at the ILU to the north of the Morum-1
331 well (Fig. 7), where the Wangerrip Group is thicker. We interpret the Morum Anticline to
332 have formed in mid-Eocene time, with the thinning of the Wangerrip Group section towards
333 the crest of the structure indicating major intra-Lutetian erosion (cf. Duddy *et al.*, 2003). The
334 absence of proven Nirranda Group sediments in the Morum-1 well, and the relatively thin
335 Heytesbury Group succession implies that the Morum Anticline has acted as a structural high
336 since the late Palaeogene.

337

338 **Copa Anticline**

339 The Copa Anticline is a structural culmination that comprises a series of small anticlines we
340 have termed Copa A-C (Fig. 2b), located ~25 km off Beachport, South Australia. Copa A and
341 B trend ~ENE-WSW and have axial traces ~6 km and ~2 km in length, respectively. Copa A
342 has an amplitude of ~100 m (Fig. 8) whilst the amplitude of Copa C is ~60 m (measured at
343 the IMU). These anticlines appear to be fault-propagation folds that formed following mild
344 reverse-reactivation of underlying normal faults. The folds trend obliquely to the dominant
345 ~NW-SE trending normal faults in the area (Fig. 2a, b), suggesting a component of dextral
346 oblique-slip reactivation. The stratigraphy in this part of the basin is constrained by the Copa-
347 1 well that was drilled in 1990 but detected no significant shows. It encountered thin
348 Heytesbury Group (~304 m) and Wangerrip Group (~105 m) successions overlying a thick
349 (~3,326 m) Sherbrook Group sequence (Fig. 3). The Wangerrip Group exhibits similar
350 thicknesses across the limbs and crests of the anticlines, and there is little evidence for onlap

351 onto the IMU indicating that these folds most likely formed subsequent to the early-
352 Palaeogene. Heytesbury Group sediments appear to thin towards and onlap the ILU (Fig. 8),
353 indicating mid-Eocene growth of Copa A and C.

354

355 The largest fold in the Copa structure is Copa B (Fig. 9). This anticline is located to the south
356 of Copa A and has a ~NW-SE orientation. The axis of this anticline is oriented sub-parallel to
357 a series of adjacent ~NW-SE trending normal faults, implying that the anticline might have
358 formed following reverse-reactivation of these faults, although the faults still exhibit net-
359 normal displacement (c.f. Williams *et al.*, 1989; Holford *et al.*, 2009b). There is some
360 evidence for onlap of reflections near the base of the Wangerrip Group onto the IMU, but the
361 largely consistent thickness of the Wangerrip Group across the fold implies that Copa C
362 formed during the late Palaeogene-Neogene, rather than the late Cretaceous-early
363 Palaeogene. Away from the crest of the anticline on its northeastern limb, late Eocene-
364 Oligocene sediments are tilted and truncated beneath the IOU, implying that folding of Copa
365 C occurred prior to the mid-Oligocene.

366

367 **Pecten Anticline**

368 The Pecten Anticline is a ~NE-SW trending fold that is ~18 km in length, and has an
369 amplitude of ~270 m measured at the IMU. Several wells that have been drilled into this
370 structure, targeting tilted syn-rift fault block traps, have discovered uncommercial (Pecten-
371 1A) and commercial (Henry-1) gas accumulations (Fig. 2c). A ~NW-SE seismic profile
372 through the Pecten Anticline reveals no evidence for onlap of Wangerrip Group, Nirranda
373 Group and Heytesbury Group sediments onto the IMU, ILU and IOU, respectively.
374 Furthermore, the thicknesses of the Wangerrip and Nirranda groups are largely consistent
375 across the fold axis. These observations indicate that the Pecten Anticline formed subsequent

376 to the Oligocene. Here the MPU is a localised angular unconformity marked by erosional
377 truncation that separates underlying tilted strata from relatively horizontal overlying strata,
378 suggesting that the folding event that formed the Pecten Anticline occurred in late Miocene-
379 early Pliocene time. Figure 10 shows clear thinning of the section between the IOU and MPU
380 towards the crest of the fold. The crest of the fold overlies the footwall of the underlying fault
381 block, implying that the Pecten Anticline might have formed through a combination of
382 differential compaction and shortening (cf. Gómez & Vergés, 2005). However, Figure 10
383 shows that the Pecten Anticline is one of several low-amplitude folds within the Cenozoic
384 succession. These folds have a wavelength of ~20 km, and not all of the folds overlie
385 Cretaceous footwall blocks. Thus whilst some of these folds may have been enhanced by
386 differential compaction, we attribute their origin to layer-parallel shortening of the Cenozoic
387 sedimentary succession

388

389 The Pecten Anticline appears to be broadly contiguous with the onshore Curdie Monocline
390 (Fig. 2c), a probable late Miocene-Pliocene compressional structure that also trends ~NW-SE
391 and has been mapped mainly from seismic sections (Tickell *et al.*, 1992). This structure is
392 indicated by a minor NW-dipping scarp, and appears to have formed above an east-dipping
393 fault, which cross-sections (Fig. 11) indicate shows reverse-offset at top Otway, Sherbrook,
394 Wangerrip and Nirranda levels (Edwards *et al.*, 1996). Clark *et al.* (2011) suggest a tentative
395 neotectonic slip rate of ~10–20 m Myr⁻¹ for this fault based on displacement of late Miocene
396 and younger stratigraphic markers.

397

398 **Minerva Anticline**

399 The Minerva Anticline is a domal structure located in the Shipwreck Trough (Fig. 2c), a ~N-
400 S trending late Cretaceous depocentre where several significant gas discoveries have been

401 made in the past few decades (Holford *et al.*, 2010b). Drilling of the Minerva-1 exploration
402 well and the Minerva-2A appraisal well into the Minerva Anticline resulted in discovery of
403 gas columns of 133 m and 111 m thickness, respectively, in Upper Cretaceous Sherbrook
404 Group (Waarre Formation) sandstone reservoirs (Geary & Reid, 1998). Our mapping
405 suggests that post-breakup growth of the Minerva Anticline is associated with the reverse-
406 reactivation of a ~E-W striking, south-dipping normal fault. The growth history of this fold
407 has previously been described by Schneider *et al.* (2004) who reported an initial, Campanian-
408 Maastrichtian phase of growth, most probably related to transpressional deformation reported
409 elsewhere in the Otway Basin at this time (Geary & Reid, 1998), and a subsequent Miocene-
410 Recent phase of deformation (Schneider *et al.*, 2004). A ~NW-SE seismic profile through the
411 anticline reveals no evidence for onlap onto the IMU or ILU, and similar to the Pecten
412 Anticline, the Wangerrip and Nirranda groups exhibit little variation in thickness across the
413 structure (Fig. 12). Folding of IOU and the observation of Heytesbury Group sediments
414 onlapping the crest of the fold constrains the timing of post-breakup compressional
415 deformation to beginning during the late Oligocene to early Miocene, consistent with the
416 previous findings of Krassay *et al.* (2004) who suggested an early-mid Miocene timing for
417 the onset of growth of the Minerva Anticline.

418

419 Similar to the offshore Pecten Anticline and the onshore Curdie Monocline, the Minerva
420 Anticline may correlate with a major onshore fold, the ~NE-SW trending Ferguson Hill
421 Anticline (Figs. 2c, 11) (Geary & Reid, 1998). However, the two folds appear to have rather
422 different growth histories (Tickell *et al.*, 1992). Stratigraphic observations suggest that
423 growth of the Ferguson Hill anticline began during the late Eocene-early Oligocene, based on
424 the patchy distribution of Nirranda Group sediments in the Ferguson Hill area (Tickell *et al.*,
425 1992). A regional unconformity at the base of the Pliocene Hanson Plain Sand implies a

426 subsequent phase of growth during the late Miocene-Pliocene (Tickell *et al.*, 1992). The
427 Pliocene deposits have themselves been folded, and Sandiford (2003a) has used
428 geomorphological evidence to suggest that the present-day topographic relief of the Ferguson
429 Hill Anticline (where Pliocene strandlines are elevated at ~245 m above sea level) might
430 largely be due to reverse-slip along ~NE-SW trending faults between ~2-1 Ma. Clark *et al.*
431 (2011) estimated tentative neotectonic slip rates of ~23–58 m Myr⁻¹ for the faults underlying
432 this structure.

433

434 **Point Ronald Anticline**

435 The Point Ronald Anticline is a ~NE-SW trending anticline located ~10 km SE of the
436 Minerva Anticline (Fig. 2c). The fold has an amplitude of ~330 m at the intra-Maastrichtian
437 unconformity, and is ~6.5 km long. As with the Pecten and Minerva anticlines, seismic data
438 through the fold show no clear evidence for onlap onto the IMU, ILU or IOU (Fig. 13). At
439 deeper levels, thinning of sediment towards a mid-Cretaceous unconformity, suggests that a
440 structural high related to compression may have existed at this location at this time. A
441 number of workers have documented evidence for a major phase of compression, uplift and
442 exhumation in the proximal Otway Ranges at ~95 Ma (Duddy, 1994; Hill *et al.*, 1995; Green
443 *et al.* 2004). The MPU forms a seabed unconformity that truncates the underlying IOU. The
444 thin sequence of post-late Oligocene sediments makes it difficult to constrain the age of the
445 structure beyond Miocene or younger.

446

447 **Crowes Anticline**

448 This ~NE-SW trending anticline is a ~20 km long fold (Fig. 2c) that has maximum amplitude
449 of ~430 m at the level of the MCU (Fig. 14). Onlap of Upper Cretaceous Sherbrook Group
450 reflectors onto the MCU suggests that, similar to the Point Ronald Anticline, a structural high

451 existed at this time, probably related to the mid-Cretaceous compression and uplift of the
452 contiguous Otway Ranges (Duddy, 1994; Hill *et al.*, 1995). Indeed, this structure correlates
453 with the onshore ~NE-SW trending Crowes Anticline (Fig. 2c), a major anticline within early
454 Cretaceous Eumeralla Formation sediments in the SW Otway Ranges that has been mapped
455 using both field observations and magnetic data (Fig. 11) (Edwards *et al.*, 1996). The IMU,
456 ILU and IOU are all folded, implying a later phase of compression, although lack of onlap
457 onto these unconformities indicates that none of them marks the timing of this compression
458 (the IMU is marked by downlap of clinofolds representing the prograding delta systems of
459 the Wangerrip Group). The MPU occurs near to the seabed, and is characterised by erosional
460 truncation of underlying strata within the Heytesbury Group. We assign a late Miocene-early
461 Pliocene age to the Cenozoic compression recorded by the Crowes Anticline. Folding most
462 likely occurred in response to reverse-slip reactivation along a deep W-dipping normal fault
463 imaged within the early Cretaceous succession (Fig. 14).

464

465 **Loch Ard Anticline**

466 The Loch Ard Anticline is a fold with a sinuous axial trace that broadly trends ~NE-SW,
467 similar to other folds in the eastern Otway Basin (Fig. 2c). Fig. 14 shows a seismic profile
468 through a ~NNW-SSE trending, ~6 km long segment of the structure that has an amplitude of
469 ~100 m at the level of the IMU. Unlike the nearby Crowes Anticline, there is no evidence for
470 onlap onto the deep mid-Cretaceous unconformity near the crest of this fold, implying that
471 the Loch Ard Anticline was not growing at this time. However, there is evidence for onlap
472 onto this unconformity on the outer limbs of the fold. In conjunction with the observation that
473 the Upper Cretaceous Sherbrook Group succession reaches its maximum thickness along the
474 axial plane, the Loch Ard Anticline appears to be a typical inversion structure, whereby a
475 former depocentre has been converted into a structural culmination (e.g. Williams *et al.*,

476 1989). There is no onlap onto the ILU or IOU, although the observation that the Wanggerip
477 Group succession encountered by the unsuccessful Loch Ard-1 well is much thinner than that
478 penetrated by nearby wells (e.g. ~132 m compared with ~456 m at Minerva-1; Fig. 3) implies
479 that the Loch Ard Anticline might have been a relative structural high throughout the Eocene.
480 However, the main phase of growth clearly occurred during the late Miocene-early Pliocene,
481 as evidenced by tilted and truncated reflections beneath the MPU.

482

483 **THE NATURE, TIMING AND DURATION OF POST-BREAKUP COMPRESSION**

484 Using a regional 2D seismic database we have constrained the Cenozoic growth history of a
485 series of compressional folds in the offshore Otway Basin (Fig. 15). The Cenozoic folds have
486 a variety of origins. Some folds, such as the Morum, Copa and Loch Ard anticlines have
487 formed following reactivation of Cretaceous normal faults. In the east of the basin where the
488 Cretaceous structural fabric broadly trends NE-SW to NNW-SSE (Fig. 2), folds such as the
489 Minerva and Loch Ard anticlines may reflect the formation of growth anticlines within
490 Cenozoic post-rift sediments due to reverse-slip reactivation of older normal faults. In the
491 west of the basin, the Cretaceous structural fabric is more dominantly E-W to WNW-ESE
492 and structures such as the Morum and Copa anticlines witness the oblique-slip reactivation of
493 syn-rift normal faults with an east-west oriented, dextral shear sense (Perineck & Cockshell,
494 1995). However, most 'inverted' faults throughout the basin retain net-normal extension, with
495 reverse-offset of syn or post-rift marker horizons rarely observed, and it is probable that most
496 Cenozoic folds have been accentuated by the buttressing of syn-rift hangingwall sediments
497 against rigid footwall blocks (cf. McClay, 1995). In addition, seismic data from the eastern
498 Otway Basin reveal evidence for low-amplitude folding of the Cenozoic succession that is
499 apparently unrelated to faulting (e.g. Fig. 10). Some of these folds may have been
500 accentuated by differential compaction over pre-rift topography, but the regular spacing of

501 these folds (wavelengths ~20 km) suggests that their origin is related to regional buckling of
502 the Cenozoic sedimentary fill in response to relatively minor amounts of shortening. The
503 increase in the amplitude of these folds from northwest to southeast within the basin is
504 consistent with estimates of Cenozoic shortening from balanced regional cross-sections,
505 which indicate negligible shortening in the western Otway Basin (e.g. Penola Trough),
506 increasing to ~5% in the eastern Otway Basin (e.g. Otway Ranges) (Cooper & Hill, 1997). A
507 basement control on Cenozoic deformation is most evident around the Otway Ranges, with
508 the orientations of the reactivated Bambra and Torquay Faults that bound the Ranges to the
509 NW and SE corresponding strongly to ~NE-SW striking structural trends in the underlying
510 Selwyn Block (Cayley *et al.*, 2002).

511

512 A summary of the timing and duration of the growth of the folds in the Otway Basin is
513 presented in Fig. 16. It is clear that post-breakup compression is not restricted to a single
514 interval of time, with the main period of deformation in the western Otway Basin occurring
515 during the mid-late Eocene (e.g. Morum and Copa), whilst in the eastern Otway Basin most
516 structures were active during the late Miocene-Pliocene (e.g. Pecten, Crowes, Loch Ard).
517 There is also evidence for Oligocene-Miocene folding in both western (e.g. Copa) and eastern
518 parts of the basin (e.g. Minerva), whilst some structures appear to have experienced multiple
519 periods of growth (e.g. Loch Ard). The onshore record of folding provides additional
520 constraints on the history of post-breakup compression. The growth histories of some onshore
521 folds appear to correlate both spatially and temporally with those we have described offshore
522 (e.g. the Pecten Anticline and Curdie Monocline, the Crowes anticlines), and some folds may
523 extend the temporal record of deformation within the basin (e.g. the Ferguson Hill Anticline
524 which has evidence for growth during the late Eocene-early Oligocene and Pleistocene).

525

526 Defining the precise duration of the increments of fold growth is difficult based on available
527 biostratigraphic constraints, but we suggest that the structures were generally active for a
528 maximum of at least >1–10 Myr before they became quiescent and the locus of deformation
529 migrated elsewhere within the basin. Palaeoseismic studies of faults with known Quaternary
530 activity onshore Australia have identified episodic slip behaviour potentially analogous to
531 that suggested for the Cenozoic structures discussed here, albeit over much shorter
532 timescales, with brief episodes of activity separated by quiescent intervals of >10–100 Kyr
533 (Crone *et al.*, 2003; Clark *et al.*, 2008; Leonard & Clark, 2011; Clark *et al.*, 2012). The
534 approximate timescales of deformation we infer from the records of fold growth in the Otway
535 Basin may represent an upper bound to the lifespan of intraplate compressional structures
536 such as the ‘active’ faults documented onshore Australia, where surficial processes
537 commonly limit the potential to constrain the extent of seismic cycles beyond the late
538 Quaternary (<130 Ka) (Crone *et al.*, 2003).

539

540 **CONSTRAINTS ON THE TIMING OF COMPRESSION FROM** 541 **THERMOCHRONOLOGICAL DATA**

542 Thermochronological data (e.g. apatite fission track analysis (AFTA), vitrinite reflectance
543 (VR), apatite (U-Th)/He dating) acquired from exploration wells that targeted Cenozoic
544 compressional structures provide further constraints on the timing of post-breakup
545 compression. AFTA and VR data from Upper Cretaceous and Cenozoic units have led to
546 identification of cooling episodes that correlate well with the timing of compression
547 established from seismic mapping.

548

549 Duddy *et al.* (2003) analysed AFTA, VR and apatite (U-Th)/He data from the Morum-1 well
550 (Fig. 17a) as part of a study into the thermal and structural history of the western Otway

551 Basin. This well drilled thin, unconformity-bound Heytesbury (~138 m) and Wangerrip
552 Group (~68 m) sequences that overlie a thick Upper Cretaceous Sherbrook Group (~1656 m)
553 succession (Duddy *et al.*, 2003). Palaeotemperatures determined from samples taken from the
554 Upper Cretaceous succession are considerably higher than the present-day temperatures in
555 the well as constrained by corrected bottom hole temperature (BHT) data (Duddy *et al.*,
556 2003). This indicates that the preserved section has been hotter in the past, and the form of
557 the palaeogeothermal gradient defined by the data implies that deeper burial by ~1.5 km of
558 now-eroded section, prior to cooling and exhumation, is the cause of the observed heating
559 (Duddy *et al.*, 2003). Combined thermal history interpretation of several AFTA and apatite
560 (U-Th)/He samples from the well suggests that the preserved Upper Cretaceous succession
561 began to cool between 57 to 40 Ma (Duddy *et al.*, 2003). This latest Palaeocene-mid Eocene
562 timing compares well with the age of the regional intra-Lutetian unconformity and is
563 consistent with the thin package of Palaeocene-age Wangerrip Group sediments preserved
564 beneath the Gambier Limestone (Duddy *et al.*, 2003). Unpublished AFTA and VR data from
565 the Copa-1 well provide similar evidence for cooling and exhumation of Wangerrip Group
566 (Dilwyn Formation) and older sediments beginning between 56 to 40 Ma (Geotrack
567 International, 2003). Thus, thermal history data provide strong independent corroboration for
568 the mid-Eocene deformation and indicate that the growth of the Morum (and likely Copa)
569 anticlines was accompanied by substantial localised exhumation.

570

571 Unpublished thermal history data for two offshore wells located in the central Otway Basin
572 (Breaksea Reef-1 and Bridgwater Bay-1; Fig. 2) was also available to this study. Both of
573 these unsuccessful wells targeted faulted late Cretaceous-age anticlines, and Bridgwater Bay-
574 1 was drilled on the southwestern edge of a large, southeasterly-plunging structural high that
575 is visible on the intra-Maastrichtian time structure map (Fig. 5c). Although there is no clear

576 evidence from seismic data for reactivation of these structures during the Cenozoic, thermal
577 history data indicates that mid-Cenozoic cooling has occurred at both locations (Fig. 16).
578 AFTA, VR and apatite (U-Th)/He data from Breaksea Reef-1 suggests that the Wangerrip
579 Group (Dilwyn Formation) and older sequences began to cool from maximum
580 palaeotemperatures ~10-20°C higher than present-day temperatures at some time in the time
581 interval 55 to 30 Ma (Geotrack International, 2003). This cooling is attributed to uplift and
582 erosion at the top-Wangerrip Group unconformity (ILU). AFTA and VR data from
583 Bridgewater Bay-1 define a period of cooling from maximum palaeotemperatures 30°C
584 higher than present-day temperatures beginning between 40 and 30 Ma (Geotrack
585 International, 2003). This well contains a major unconformity that separates the mid-Eocene
586 Nirranda Group from the overlying Miocene Port Campbell Limestone Formation (IOU).
587 This unconformity is characterised on seismic data by truncation and downlap, and the AFTA
588 and VR results are interpreted as recording significant erosion of the underlying Nirranda
589 Group at the IOU (Geotrack International, 2003).

590

591 In the eastern Otway Basin, published palaeotemperature data from exploration wells and
592 outcrops around the Otway Ranges are generally dominated by younger, late Cenozoic
593 cooling (Duddy, 1997; Cooper & Hill, 1997; Green *et al.*, 2004; Holford *et al.*, 2011b),
594 consistent with the predominance of younger (i.e. Miocene–Pliocene) fault reactivation and
595 folding in this part of the basin. AFTA, VR and apatite (U-Th)/He data from the Nerita-1 well
596 (Fig. 17b) in the contiguous Torquay sub-basin indicate that the development of the Nerita
597 Anticline, a major ~NE-SW trending inversion structure commenced between 10 and 5 Ma
598 (Fig. 18) (Holford *et al.*, 2011b), in excellent agreement with stratigraphic constraints
599 provided by dating of the regional late Miocene-early Pliocene unconformity (Dickinson *et*
600 *al.*, 2002). These data also indicate that the growth of the Nerita Anticline was accompanied

601 by ~1 km of erosion (Fig. 17b) (Holford *et al.*, 2011b). AFTA, VR and apatite (U-Th)/He
602 data from the nearby, onshore Anglesea-1 reveal similar evidence for significant exhumation
603 (removing up to 750–950 m of Eocene-Miocene section) beginning in the late Miocene
604 (between 12 to 7 Ma) (Green *et al.*, 2004). Both onshore and offshore in the Torquay sub-
605 basin there is also evidence for older periods of post-breakup deformation, particularly during
606 the mid-Eocene (Trupp *et al.*, 1994; Holdgate *et al.*, 2001).

607

608 Of the eastern Otway Basin compressional structures described in this study, the early-mid
609 Miocene-age Minerva Anticline has the most comprehensive published thermal history
610 dataset. Holford *et al.* (2010b) presented AFTA and VR data from Upper Cretaceous
611 Sherbrook Group and Lower Cretaceous Otway Group samples recovered from the Minerva-
612 1 exploration well (Fig. 17c). Palaeotemperatures estimated from these data are highly
613 consistent with the present-day temperatures in the well constrained by BHT data, indicating
614 that the preserved section is currently at or close to maximum post-depositional temperatures,
615 and thus prohibiting independent timing constraints from thermal history data. In contrast to
616 the Nerita and Morum anticlines, the growth of the Minerva Anticline accompanied by
617 relatively minor coeval exhumation (<300 m), which may reflect deeper bathymetry during
618 development of the latter structure (Holford *et al.*, 2010b). A study of AFTA and VR data
619 from the La Bella-1 and Mussel-1 wells located on the Mussel Platform, approximately ~25
620 km to the south of the Minerva Anticline, indicated substantial localized exhumation
621 beginning around 60 Ma, during which up to 1.5 km of section was removed (Duddy &
622 Erout, 2001). This ‘pre-breakup’ exhumation is attributed to localized transpression during
623 the opening of the Southern Ocean, which involved a significant component of left-lateral
624 shear (Schneider *et al.*, 2004).

625

626 **DRIVING MECHANISMS BEHIND POST-BREAKUP COMPRESSION IN THE**
627 **OTWAY BASIN**

628 **Insights from contemporary stress data**

629 The increasing recognition of post-breakup deformation along rifted continental margins has
630 motivated numerous studies into the mechanisms that control such unanticipated tectonic
631 activity, and a wide range of causal processes have consequently been invoked. These include
632 the transmission of compressional stresses from active orogenic zones (Cobbold *et al.*, 2001;
633 Ziegler *et al.*, 1995); topographic body forces such as ridge-push (Bott, 1993; Doré *et al.*
634 2008) or resulting from topographic gradients at continental margins (Pascal & Cloetingh,
635 2009); reactivation of basement lineaments (Lundin & Doré, 1996; Hudec & Jackson, 2002);
636 and differential seafloor spreading and mantle drag (Mosar *et al.*, 2002; Le Breton *et al.*,
637 2012).

638
639 It is generally understood that the Quaternary-contemporary deformation of continental
640 Australia and its rifted margins is controlled, to first-order, by a complex intraplate stress
641 field generated by distant plate boundary interactions (Reynolds *et al.*, 2002; Sandiford,
642 2003b; Sandiford *et al.*, 2004; Hillis *et al.*, 2008b). Several key lines of evidence support this
643 view. Present-day maximum horizontal stress orientations across Australia, measured using
644 earthquake focal mechanisms, borehole breakouts and drilling-induced tensile fractures
645 (DITFs), indicate consistent stress orientations within individual regions and basins, but
646 considerable variation from region-to-region across the continent (Fig. 1) (Hillis & Reynolds,
647 2000). This complex pattern of intraplate stress orientations contrasts strongly with
648 comparable continental regions (e.g. western Europe; Gölke & Coblenz, 1996), which tend
649 to show maximum horizontal stress orientations that broadly parallel the direction of plate
650 motion. Independent studies of Quaternary-contemporary faulting across Australia indicate

651 that the strikes of many of the identified structures are broadly orthogonal to the present-day
652 stress orientations determined in specific regions (Sandiford, 2003b; Quigley *et al.*, 2006;
653 Hillis *et al.*, 2008b). It is notable that, where reliable kinematic constraints are available,
654 onshore Quaternary faults generally indicate dip-slip or oblique-slip reverse motions, and no
655 faults with demonstrable motions that are purely strike-slip or normal have been documented
656 as yet (Hillis *et al.*, 2008b).

657

658 Despite the evidently complicated pattern of contemporary stress orientations across
659 Australia, valuable insights into the origins of this stress field have been obtained from two-
660 dimensional, elastic finite element modelling applied to the Indo-Australian Plate (Coblentz
661 *et al.*, 1998; Reynolds *et al.*, 2002; Sandiford *et al.*, 2004). These models have achieved
662 excellent statistical fits between observed and predicted stress orientations by focussing the
663 distributed ‘ridge-push’ plate-driving torques related to the SW boundary of the Indo-
664 Australian Plate against the collisional segments of the complex convergent NE plate
665 boundary that act as sources of resistance (i.e. Himalayas, New Guinea, New Zealand) (Hillis
666 *et al.*, 2008b; Sandiford & Quigley, 2009). The excellent agreement between observed
667 present-day stress patterns and those predicted from modelling studies lends strong credence
668 to the notion that plate boundary forces exert the primary control upon the contemporary
669 stress field, and thus deformation, of Australia and its margins. An important corollary of this
670 premise is that, although individual plate boundaries and their associated driving or resisting
671 torques unquestionably exert a profound influence on the state of stress within the plate
672 interior, in the case of Australia at least, both the contemporary stress and deformation fields
673 cannot be attributed to a single plate boundary force or event.

674

675 Present-day maximum horizontal stress orientations in the Otway Basin have been well-
676 constrained using borehole breakouts and drilling induced tensile fractures (DITFs)
677 interpreted from petroleum wells (Hillis *et al.*, 1995; Nelson *et al.*, 2006). Maximum
678 horizontal stress orientations are generally oriented NW-SE, with data revealing a slight
679 anticlockwise rotation from $\sim 125^\circ\text{N}$ in the western (SA) Otway Basin, to $\sim 135^\circ\text{N}$ in the east
680 (Victoria) (Fig. 15) (Nelson *et al.*, 2006). Farther to the east, in the Gippsland Basin, there is
681 additional rotation of the maximum horizontal stress orientation to $\sim 139^\circ\text{N}$ (Nelson *et al.*,
682 2006). The broad \sim NW-SE strike directions of the majority of the anticlines documented in
683 this study are thus consistent with independently determined present-day stress orientations,
684 implying that post-breakup deformation in the Otway Basin has been controlled by plate-
685 boundary forces.

686

687 There is less certainty regarding stress magnitudes and the nature of the stress contemporary
688 regime in the Otway Basin. The neotectonic record, particular from the eastern Otway Basin,
689 favours a reverse-fault stress regime (i.e. $\sigma_{\text{H}} > \sigma_{\text{h}} > \sigma_{\text{v}}$) (Sandiford *et al.*, 2004; Hillis *et al.*,
690 2008b), but petroleum data from wells located throughout the basin suggest a strike-slip fault
691 stress regime (i.e. $\sigma_{\text{H}} > \sigma_{\text{v}} > \sigma_{\text{h}}$) (Nelson *et al.*, 2006). Using density logs to calculate vertical
692 stress magnitudes, leak-off tests to constrain minimum horizontal stress and DITFs to
693 calculate maximum horizontal stress magnitudes, Nelson *et al.* (2006) found the state-of-
694 stress to be strike-slip in both the SA and Victorian parts of the Otway Basin. Their analysis
695 revealed increases in both minimum and maximum horizontal stress magnitudes from
696 western to eastern parts of the basin (minimum horizontal stress increasing from $\sim 15.5 \text{ MPa}$
697 km^{-1} to $\sim 18.5 \text{ MPa km}^{-1}$; maximum horizontal stress increasing from $\sim 29 \text{ MPa km}^{-1}$ to ~ 37
698 MPa km^{-1}). The high magnitude of minimum horizontal stress observed in the eastern Otway

699 Basin suggests that the state-of-stress is approaching a reverse fault stress regime (Nelson *et*
700 *al.*, 2006).

701

702 Several previous studies have interpreted the record of Cenozoic deformation along the
703 eastern parts of the southern Australian margin in terms of an E-W orientated dextral strike-
704 slip regime that resolves into ~NW-SE directed compression (Perineck & Cockshell, 1995;
705 Jensen-Schmidt *et al.*, 2002; Pollock, 2003), consistent with present-day maximum horizontal
706 stress orientations in the Otway Basin inferred from petroleum data (Hillis *et al.*, 1995;
707 Nelson *et al.*, 2006). A dextral strike-slip regime can account for the formation of ~NW-SE
708 oriented anticlines that form under compression, or through transpressional shortening during
709 the reactivation of ~WNW-ESE oriented normal faults, such as those which dominate the
710 structural grain in the western Otway Basin (e.g. around the Morum and Copa anticlines).

711

712 However, a recent reanalysis of stress magnitude data from the Otway Basin (King *et al.*,
713 2012) using a new method for evaluating leak-off test results that assumes shear failure of
714 pre-existing fractures under compressional stress regimes (Couzens-Schultz & Chan, 2010)
715 suggests that the present-day state-of-stress in the Otway Basin is better characterized by a
716 reverse-fault stress regime than the strike-slip fault stress regime proposed in earlier studies
717 (e.g. Hillis *et al.*, 1995; Nelson *et al.*, 2006). Such a stress regime would appear to be more
718 compatible with the neotectonic faulting record from southern Australia, and with
719 independent constraints on the state-of-stress from earthquake focal mechanism solutions
720 (Hillis *et al.*, 2008b).

721

722

723

724 Linking post-breakup compression to evolving plate boundary forces

725 The recognition of spatially and temporally migrating post-breakup deformation in the Otway
726 Basin is one of the key outcomes of this study. Figure 16 depicts a chronology of the timing
727 and duration of activity for the structures we have identified. This confirms that deformation
728 within the basin has been common following breakup, but is mainly concentrated into several
729 periods of enhanced deformation when growth is evident on multiple structures within the
730 basin. Here we discuss the significance of these enhanced periods of deformation, which
731 occurred during the mid-Eocene and the late Miocene-early Pliocene. During the latter there
732 is evidence for active growth of the Pecten, Ferguson Hill, Point Ronald, Crowes and Loch
733 Ard anticlines in the Otway Basin (Fig. 16), the Nerita Anticline in the adjacent Torquay sub-
734 basin (Holford *et al.*, 2010b, 2011b), and multiple onshore neotectonic faults that displace
735 late Miocene-Quaternary sedimentary and volcanic rocks (Clark *et al.*, 2012). The growth of
736 these structures is coeval with the development of a widespread low-angle unconformity that
737 is dated as between 10 and 5 Myr old, and occurs over a distance of ~1000 km along the
738 southern Australian margin, from the Gulf St Vincent Basin in the NW to the Gippsland
739 Basin in the SE (Dickinson *et al.*, 2001, 2002; Sandiford *et al.*, 2004).

740

741 In an investigation into the causes of neotectonic activity in southeastern Australia, Sandiford
742 *et al.* (2004) concluded that the origin of the present-day stress field in this part of the
743 Australian continent can be traced back to the terminal Miocene or early Pliocene (~10–5
744 Ma). They argued that a significant change in the state-of-stress occurred at this time in
745 response to concomitant changes in the coupling of the Indo-Australian and Pacific plates
746 following the building of the Southern Alps in New Zealand, from ~12 Ma onwards
747 (Sandiford *et al.*, 2004). They illustrated the considerable influence of the New Zealand plate
748 boundary segment on the southeastern Australian stress regime through the use of finite

749 element models similar to those constructed by Reynolds *et al.* (2002). Their modelling
750 results indicate that in the absence of any transmission of force from the New Zealand
751 boundary to the plate, maximum horizontal stress orientations in the Otway and Gippsland
752 basins would most likely have ~NE-SW-trending azimuths. With increasing magnitudes of
753 collisional force, modelled maximum horizontal stresses progressively rotate to ~NW-SE
754 orientations that are consistent with both present-day stress data and the strikes of the post-
755 breakup deformation structures documented herein. These results also suggest that the
756 observed anticlockwise rotation of maximum horizontal stress that occurs between the
757 western Otway (~125°N) and Gippsland basins (~139°N) can be understood in terms of
758 relative proximity to the New Zealand boundary, which may also control the increase in
759 minimum and (inferred) maximum horizontal stress magnitudes towards eastern parts of the
760 southern margin (Sandiford *et al.*, 2004; Nelson *et al.*, 2006).

761

762 It is important to acknowledge that important changes to the nature of the Indo-Australian
763 plate boundary zones in late Miocene-early Pliocene time were not restricted to the New
764 Zealand region. As summarised by Hillis *et al.* (2008b), this period witnessed the collision
765 between the Ontong Java Plateau and the Solomon Arc (Wessel & Kroenke, 2000), the
766 initiation of compressional deformation in the Indian Ocean (Krishna *et al.*, 2001) and the
767 onset of transpressional deformation and uplift in New Guinea (Hill & Hall, 2003). The latter
768 deformation event, which occurred some 3500 km to the north of this study area, has
769 previously been invoked as the key incident responsible for post-breakup deformation in the
770 Otway Basin (Hill *et al.*, 1995).

771

772 Our preferred explanation for the late Miocene-early Pliocene deformation pulse, based on
773 the insights obtained from finite element modelling of the contemporary Australian stress

774 field (e.g. Reynolds *et al.*, 2002; Müller *et al.*, 2012), is that it represents an intraplate
775 response to the reconfigurations of the Indo-Australian Plate boundaries which all combine to
776 influence the balance of forces within the plate. However, the recognition of Eocene to early-
777 Miocene age post-breakup structures striking ~NE-SW shows that the ~NW-SE σ_H
778 orientation is a more persistent feature than proposed by Sandiford *et al.* (2004), who
779 suggested that this stress orientation was initiated at ~12 Ma by increased coupling of the
780 Australian-Pacific plate boundary. This observation implies that factors other than the
781 Miocene evolution of the Australian-Pliocene plate boundary must be responsible for the
782 ~NW-SE σ_H orientation, though it remains possible that the late Miocene-early Pliocene
783 deformation pulse reflects a significant increase in stress magnitudes resulting from the
784 enhanced forcing from New Zealand (Sandiford *et al.*, 2004).

785

786 The second period of enhanced post-breakup deformation that merits discussion occurred
787 during the mid-Eocene. In the western Otway Basin, this time interval witnessed significant
788 growth on the Morum and Copa anticlines (Figs. 15, 16) as indicated by mapping of a
789 regionally extensive intra-Lutetian unconformity, and supported by thermochronological data
790 which record substantive localised exhumation in the vicinity of these structures (Duddy *et*
791 *al.*, 2003). In the eastern Otway Basin there is evidence that the Loch Ard Anticline
792 underwent uplift at this time based on observed thinning of the Wangerrip Group across this
793 structure. There is also evidence for mid-Eocene fault reactivation in the Port Campbell
794 Embayment from structural mapping of onshore 3D seismic data (P. Boulton personal
795 communication), and folding associated with the intra-Lutetian unconformity has been shown
796 to occur both offshore and onshore in the adjacent Torquay sub-basin (Trupp *et al.*, 1994;
797 Holdgate *et al.*, 2001). Given the pervasive extent of mid-Eocene deformation, it may be the
798 case that neotectonic faults for which only late Miocene-onwards displacements can be

799 confidently demonstrated (Clark *et al.*, 2012), may have also accrued slip during the mid-
800 Eocene (and/or Oligocene-early Miocene).

801

802 The Morum Anticline strikes ~NE-SW, consistent with the orientations of structures active
803 during the late Miocene-early Pliocene (and those active during the Oligocene-early
804 Miocene; Fig. 15), implying that maximum horizontal stress in the basin has broadly trended
805 ~NW-SE for the past ~45 Ma. The folds that comprise the Copa Structure have varying
806 trends including ~NNE-SSW and ~NW-SE, but the structure is generally consistent with
807 having formed by oblique-slip reactivation of normal faults under ~NW-SE directed
808 compression.

809

810 Our best estimate for the timing of enhanced deformation during the mid-Eocene based on
811 stratigraphic constraints and mapping of individual structures is ~45 to 38 Ma. In a similar
812 fashion to the subsequent phase of basin-wide deformation during the late Miocene-early
813 Pliocene, fault-reactivation and folding during the mid-Eocene was also contemporaneous
814 with major plate boundary reconfigurations. Most relevant in terms of the evolution of the
815 southern margin, final plate separation between Australia and Antarctica is thought to have
816 been achieved by ~43 Ma (Norvick & Smith, 2001). Breakup marked the onset of fast
817 spreading in the Southern Ocean, with half-spreading rates along the Great Australian Bight
818 ridge system accelerating from $<0.5 \text{ cm yr}^{-1}$ prior to 43 Ma, to 3.3 cm yr^{-1} by 34 Ma (Li *et al.*,
819 2003). Several other significant plate boundary adjustments took place at approximately 43
820 Ma, including an acceleration and ~70° counter clockwise rotation of motion of the Pacific
821 Plate, and the abandonment of the eastern Indian Ocean spreading ridge leading to the fusing
822 of the Indian and Australian plates (Veevers, 2000). These events, which followed the
823 cessation of spreading in the Tasman Sea at ~52 Ma (Gaina *et al.*, 1998) and accompanied the

824 deceleration of the Indian Plate during the nascent stages of Himalayan collision (Patriat &
825 Achache, 1984), conspired to establish a compressional stress regime within the Australian
826 crust dominated by ridge push to the south of Australia and increased resisting forces to the
827 north (Dyksterhuis & Müller, 2008; Sandiford & Quigley, 2009; Müller *et al.*, 2012). We
828 submit that the mid-Eocene shortening in the Otway Basin and adjacent parts of the southern
829 margin represents an intraplate response to the initiation of a compressional stress regime
830 within the Indo-Australian Plate shortly after breakup.

831

832 **COMPARISONS WITH THE RECORD OF POST-BREAKUP DEFORMATION AT** 833 **THE NW EUROPEAN ATLANTIC RIFTED MARGIN**

834 We conclude this discussion with a brief comparison between the records of post-breakup
835 deformation at the southern Australian margin and NW European Atlantic margin, which
836 contains the best-documented record of post breakup deformation at a rifted continental
837 margin. The NW European margin formed following multiple Permian to Paleogene rifting
838 episodes, with continental breakup between NW Europe and Greenland achieved by ~53.7
839 Ma (Doré *et al.*, 2008). The post-breakup sedimentary record of the margin is dominated by
840 multiple, Eocene and younger, siliclastic sediment wedges that prograde from the continental
841 shelves of the British Isles, Norway and Faroe Islands, accompanied by the deposition of
842 deep-water contourites in the adjacent basins since late Eocene time (Stoker *et al.*, 2010).
843 Previous studies have documented widespread compressional folding on the Rockall-Faroes-
844 West Shetland and mid-Norwegian sections of this margin, with particularly intense phases
845 of deformation identified during the mid-Eocene to Oligocene and early-mid Miocene
846 (Boldreel and Anderson, 1998; Lundin and Doré, 2002; Stoker *et al.*, 2005).

847

848 Major post-breakup structures on the mid-Norwegian margin are generally located within the
849 Vøring Basin, with compressional features largely absent from the adjacent Møre Basin and
850 Halten Terrace (Doré *et al.*, 2008). The structures comprise large-scale, elongate anticlines
851 with four-way dip closure and low amplitude/wavelength ratios that mostly trend ~NE-SW to
852 N-S (Gómez & Vergés, 2005). The largest structures include the Ormen Lange Dome and
853 Helland-Hansen Arch, the latter of which has an amplitude of ~1 km and axial trace length of
854 ~200 km (Doré *et al.*, 2008). Both these structures have documented mid-Eocene-early
855 Oligocene growth phases and were reactivated during the early-mid Miocene when other
856 folds including the Vema, Hedda, and Naglfar domes also developed (Lundin and Doré,
857 2002). Though some structures such as the Helland Hansen Arch appear to be related to the
858 reactivation of normal fault systems, many of the structures do not appear to be directly
859 linked to underlying faults (Doré *et al.*, 2008). Whilst a compressional origin of these
860 structures is generally agreed (Doré *et al.*, 2008), shortening magnitudes appear to be minor
861 (a few percent) (Våagnes *et al.*, 1998) and in many cases the amplitudes of folds have been
862 enhanced by sedimentation and differential compaction on their flanks (Gómez & Vergés,
863 2005).

864

865 Post-breakup structures in the Rockall-Faroes-West Shetland area also mostly comprise folds
866 that exhibit a wide variation in scale (axial trace lengths <10 to >250 km), orientation and
867 timing of growth (Ritchie *et al.*, 2008). The largest structures include the Fugloy,
868 Munkagrunnur and Wyville Thomson ridges, which form prominent bathymetric highs with
869 reliefs of ≤ 900 m (Stoker *et al.*, 2005). Seismic mapping reveals significant early-mid
870 Miocene growth of these structures (Stoker *et al.*, 2005), but also reveals long-lived growth
871 of the latter throughout the Eocene-Oligocene (Ritchie *et al.*, 2008). Other structures with
872 long-lived growth histories include the North Hatton Bank Fold Complex on the Hatton High

873 (mid-Eocene to early Oligocene). In the NE Faeroe-Shetland Basin there are numerous NE-
874 SW and NNE-SSE trending growth folds that developed in the early-mid Miocene and early
875 Pliocene, and some of the younger structures have associated raised seabed profiles
876 suggesting ongoing compression (Ritchie *et al.*, 2008).

877

878 In comparison to the NW European Atlantic margin, both the quantity and dimensions of
879 post-breakup structures along the southern Australian margin are smaller (Tuitt *et al.*, 2011).
880 However, at both margins the orientations of paleostresses inferred from compressional
881 structures are highly consistent with independent determinations of the present-day stress
882 field. Post-breakup structures on the NW European margin exhibit larger variation in
883 orientation, which at least partially reflects the protracted and complex rifting history of this
884 margin and the influence of syn-breakup magmatism (Ritchie *et al.*, 2008). Fold trends show
885 most consistency in the Faeroe-Shetland Basin (mostly ~NE-SW) and offshore Norway
886 (broadly ~N-S), and paleostress orientations from these structures are also largely consistent
887 with the observed ~NW-SE present-day maximum horizontal stress orientation (Gölke and
888 Coblentz, 1996). Furthermore, both margins display similarities in the chronology of
889 deformation, with clear periods of enhanced compressional activity (e.g. early-mid Miocene
890 in NW Europe, late Miocene-early Pliocene in southern Australia), but fold growth has taken
891 place over extended periods at both margins following breakup. Doré *et al.* (2008) suggest
892 that the mid-Miocene acme of deformation along the NW European margin can be explained
893 by enhanced body forces, and thus intraplate stress magnitudes, resulting from development
894 of the Iceland insular margin on the North Atlantic ridge-system during the middle Miocene.
895 This enhanced ridge-push forcing, combined with the presence of hyperextended and
896 weakened lithosphere (Lundin & Doré, 2011), may account for the larger dimensions of post-
897 breakup structures on the NW European margin.

898 **CONCLUSIONS**

899 Seismic mapping in the offshore Otway Basin has identified a number of post-breakup
900 compressional structures in this supposedly ‘passive’ rifted margin setting. Individual
901 structures have a variety of ages but taken as a whole, the evidence presented here shows that
902 the Otway Basin has been subject to continual compressional forcing subsequent to breakup,
903 with strain migrating spatially and temporally within the basin and often reactivating syn-
904 breakup fault systems. However, most post-breakup compressional activity is concentrated
905 into two periods of enhanced deformation during the mid-Eocene and late Miocene-Pliocene.
906 Our findings have important implications for the understanding of ‘passive’ margin tectonism
907 and for the evolution of intraplate stress fields. Unanticipated deformation of ‘passive’
908 margins has been increasingly documented as petroleum exploration progressively focuses on
909 deep-water basins along continental shelves worldwide (e.g. Cobbold *et al.*, 2001; Hudec &
910 Jackson, 2002; Doré *et al.*, 2008). Attempts to explain such deformation have frequently
911 focused on the episodic nature of post-breakup fault-reactivation, folding and uplift, and have
912 attempted to link periods of tectonic activity with far-field events at plate boundaries (e.g.
913 Ziegler *et al.*, 1995; Holford *et al.*, 2009a).

914

915 The chronology of post-breakup deformation that we have established does indeed reveal
916 several periods of enhanced fault-reactivation and folding, occurring immediately after mid-
917 Eocene breakup and subsequently during the late Miocene-early Pliocene, though growth on
918 some important structures has clearly occurred outside of these time intervals, suggesting that
919 post-breakup compression may be more common than is generally assumed. The key periods
920 of enhanced post-breakup deformation clearly correlate with significant events at proximal
921 Indo-Australian Plate boundaries (e.g. final Australia-Antarctica plate separation and onset of
922 fast spreading in the mid-Eocene, development of the Southern Alps along the New Zealand

923 plate boundary segment), and these events should be viewed in terms of larger-scale
924 reconfigurations of the Indo-Australian Plate boundaries that occurred at these times. These
925 reconfigurations served to establish a compressional stress regime within the plate interior,
926 with contemporary Australia characterised by unusually high levels of seismicity for a
927 continental region far from plate boundaries, and demonstrably high horizontal stress
928 magnitudes in the upper crust (Hillis *et al.*, 2008b; Sandiford & Quigley, 2009).

929

930 We believe that the record of post-breakup deformation in the Otway Basin can be
931 understood best in terms of the responses of the passive margin sedimentary succession and
932 rift-related fault-systems to a continuously evolving compressional stress field that is coupled
933 with, and controlled by, the progressive evolution of plate boundaries and their associated
934 driving or resisting forces. Periods of enhanced basin-wide deformation are likely related to
935 step changes in the intraplate stress regime (i.e. magnitudes and/or orientations) resulting
936 from significant modifications in the nature or disposition of one or more plate boundary
937 segments. This theory appears to be consistent with the record of post-breakup deformation
938 along the NW European Atlantic passive margin, which contains similar evidence for
939 protracted fault-reactivation and folding since ~53 Ma, but with periods of widespread
940 compression in discrete time intervals that coincide with fundamental changes in plate
941 boundary forcing (Doré *et al.*, 2008; Ritchie *et al.*, 2008; Holford *et al.*, 2009a). To obtain
942 further insights into the nature and origin of post-breakup deformation at rifted margins, it
943 will be necessary to compare the records of the southern Australian and NW European
944 margins with deformation chronologies obtained at other passive margins that appear to be
945 uncharacteristically active, such as the conjugate margins of the South Atlantic Ocean (e.g.
946 Cobbold *et al.*, 2001; Hudec & Jackson, 2002; Turner *et al.*, 2008).

947

948 **ACKNOWLEDGEMENTS**

949 This publication was supported by ARC Discovery Project DP0897612, and forms TRaX
950 record #264. We gratefully acknowledge PGS for their generous donation of the Southern
951 Australian Margin Digital Atlas, DMITRE and DPI Victoria for access to additional seismic
952 data, and SMT/IHS for provision of KINGDOM. We thank Chris Jackson for editorial
953 assistance, reviewers Tony Doré and Jaume Vergés for their constructive feedback, and
954 colleagues in the S³ Research Group for useful discussions on the stress and neotectonics of
955 southeastern Australia. MSS publishes with the permission of the Executive Director, British
956 Geological Survey (Natural Environment Research Council).

957

958 **REFERENCES**

959 BERNECKER, T., SMITH, M.A., HILL, K.A. & CONSTANTINE, A.E. (2003) Oil and gas,
960 fuelling Victoria's economy. In: *Geology of Victoria* (Ed. by W.D. Birch), *Geol. Soc. Aust.*,
961 *Spec. Publ.*, 23, 469-487.

962

963 BLEVIN, J. & CATHRO, D. (2008) Australian Southern Margin Synthesis. *Client report to*
964 *Geoscience Australia by FrOG Tech Pty Ltd*. Project GA707,

965

966 BOLDREEL, L.O. & ANDERSEN, M.S. (1998) Tertiary compressional structures on the
967 Faroe-Rockall Plateau in relation to northeast Atlantic ridge-push and Alpine foreland
968 stresses. *Tectonophys.* 300, 13-28.

969

970 BOND, G.C. & KOMINZ, M.A. (1988) Evolution of thought on passive continental margins
971 from the origin of geosynclinal theory (~1860) to the present. *Geol. Soc. Am., Bull.*, 100,
972 1903-1933.

- 973 BOTT, M.H.P. (1993) Modelling the plate-driving mechanism. *J. Geol. Soc.*, 150, 941-951.
974
- 975 BOULT, P.J., WHITE, M.R., POLLOCK, R., MORTON, J.G.G., ALEXANDER, E.M. &
976 HILL, A.J. (2002) Chapter 6: Lithostratigraphy and environments of deposition. In:
977 *Petroleum Geology of South Australia. Vol. 1: Otway Basin, Second Edition.* (Ed. by P.J.
978 Boulton and J.E. Hibbert).
- 979
- 980 BRAUN, J. (2010) The many surface expressions of mantle dynamics. *Nat. Geosci.*, 3, 825-
981 833.
982
- 983 BROWN, B.R. (1986) Offshore Gippsland Silver Jubilee. In: *Second South-Eastern Australia*
984 *Oil Exploration Symposium, Melbourne* (Ed. by R.C.Glenie), pp. 29–56. The Petroleum
985 Exploration Society of Australia Victoria and Tasmanian Branch, Canberra, Australia.
986
- 987 CAYLEY, R.A., TAYLOR, D.H., VANDENBERG, A.H.M. & MOORE, D.H. (2002)
988 Proterozoic-early Palaeozoic rocks and the Tyennan Orogeny in central Victoria: the Selwyn
989 Block and its tectonic implications. *Aust. J. Earth Sci.*, 49, 225-254.
990
- 991 CÉLÉRIER, J., SANDIFORD, M., HANSEN, D.L. & QUIGLEY, M. (2005) Modes of
992 active intraplate deformation, Flinders ranges, Australia. *Tectonics*, 24,
993 10.1029/2004TC001679.
994
- 995 CLARK D., DENTITH M., WYRWOLL K.H., YANCHOU L., DENT V. &
996 FEATHERSTONE, C. (2008) The Hyden fault scarp, Western Australia: paleoseismic

- 997 evidence for repeated Quaternary displacement in an intracratonic setting. *Aust. J. Earth Sci.*,
998 55, 379-395.
- 999
- 1000 CLARK, D., McPHERSON, A. & COLLINS, C.D.N. (2011) *Australia's seismogenic*
1001 *neotectonic record: a case for heterogeneous intraplate deformation*. Record 2011/11,
1002 Geoscience Australia, Canberra.
- 1003
- 1004 CLARK, D., McPHERSON, A. & VAN DISSEN, R. (2012) Long-term behaviour of
1005 Australian stable continental region (SCR) faults. *Tectonophysics*, 566-567, 1-30.
- 1006
- 1007 COBBOLD, P.R., MEISLING, K. & MOUNT, V. S. (2001) Reactivation of an obliquely
1008 rifted margin, Campos and Santos basins, southeastern Brazil. *AAPG Bull. (Am. Assoc.*
1009 *Petrol. Geol.)*, 85, 1925-1944.
- 1010
- 1011 COBBOLD, P.R., ROSSELLO, E.A., ROPERCH, P., ARRIAGADA, C., GÓMEZ, L.A. &
1012 LIMA, C. (2007) Distribution, timing, and causes of Andean deformation across South
1013 America. In: *Deformation of the Continental Crust: The Legacy of Mike Coward* (Ed. by
1014 A.C. Ries, R.W.H. Butler and R.H. Graham), *Geol. Soc. Spec. Publ.*, 272, 321-343.
- 1015
- 1016 COBBOLD, P.R., GILCHRIST, G., SCOTCHMAN, I., CHIOSSI, D., FONSECA CHAVES,
1017 F., GOMES DE SOUZA, F. & LILLETVEIT, R. (2010) Large submarine slides on a steep
1018 continental margin (Camamu Basin, NE Brazil). *J. Geol. Soc.*, 167, 583-592.
- 1019

- 1020 COBLENTZ, D.D., ZHOU, S., HILLIS, R.R., RICHARDSON, R.M. & SANDIFORD, M.
1021 (1998) Topography, boundary forces, and the Indo-Australian intraplate stress field. *J.*
1022 *Geophys. Res.*, 103, 919–931.
- 1023
- 1024 COOPER, G.T. & HILL K.C. (1997) Cross-section balancing and thermochronological
1025 analysis of the Mesozoic development of the eastern Otway Basin. *APPEA J.*, 37, 390-414.
- 1026
- 1027 COUZENS-SCHULTZ, B.A. & CHAN, A.W. (2010) Stress determination in active thrust
1028 belts: An alternative leak-off pressure interpretation. *J. Struct. Geol.*, 32, 1061-1069.
- 1029
- 1030 CRONE, A.J., DE MARTINI, P.M., MACHETTE, M.N., OKUMURA, K. & PRESCOTT,
1031 J.R. (2003) Paleoseismicity of two historically quiescent faults in Australia: Implications for
1032 fault behaviour in stable continental regions. *Bull. Seis. Soc. Am.*, 93, 1913-1934.
- 1033
- 1034 DAVIES, R., CLOKE, I., CARTWRIGHT, J., ROBINSON, A. & FERRERO, C. (2004)
1035 Post-breakup compression of a passive margin and its impact on hydrocarbon prospectivity:
1036 An example from the Tertiary of the Faeroe–Shetland Basin, United Kingdom. *AAPG Bull.*
1037 *(Am. Assoc. Petrol. Geol.)*, 88, 1-20.
- 1038
- 1039 DENHAM, D., WEEKES, J. & KRAYSHEK, C. (1981) Earthquake evidence for
1040 compressive stress in the southeast Australian crust. *Aust. J. Earth Sci.*, 28, 323-332.
- 1041
- 1042 DICKINSON, J.A., WALLACE, M.W., HOLDGATE, G.R., DANIELS, J., GALLAGHER,
1043 S.J. & THOMAS, L. (2001) Neogene tectonics in SE Australia: implications for petroleum
1044 systems. *APPEA J.*, 41, 37-52.

- 1045 DICKINSON, J.A., WALLACE, M.W., HOLDGATE, G.R., GALLAGHER, S.J. &
1046 THOMAS, L. (2002) Origin and timing of the Miocene-Pliocene unconformity in southeast
1047 Australia. *J. Sed. Research*, 72, 288–303.
- 1048
- 1049 DORÉ, A.G., CORCORAN, D.V. & SCOTCHMAN, I.C. (2002) Prediction of the
1050 hydrocarbon system in exhumed basins, and application to the NW European margin. In:
1051 *Exhumation of the North Atlantic Margin: Timing, Mechanisms and Implications for*
1052 *Petroleum Exploration* (Ed. by A.G. Doré, J.A. Cartwright, M.S. Stoker, J.P. Turner & N.
1053 White), *Geol. Soc. Spec. Publ.*, 196, 401-429.
- 1054
- 1055 DORÉ, A.G., LUNDIN, E.R., KUSZNIR, N.J. & PASCAL, C. (2008) Potential mechanisms
1056 for the genesis of Cenozoic domal structures on the NE Atlantic margin: pros, cons, and some
1057 new ideas. In: *The Nature and Origin of Compression in Passive Margins* (Ed. by H.
1058 Johnson, A.G. Doré, R.W. Gatliff, R. Holdsworth, E.R. Lundin, and J.D. Ritchie), *Geol. Soc.*
1059 *Spec. Publ.*, 306, 1-26.
- 1060
- 1061 DUDDY, I.R. (1994) The Otway Basin: thermal, structural and tectonic and hydrocarbon
1062 generation histories. In: *NGMA/PESA Otway Basin Symp.*, (Ed. by D.M. Finlayson), AGSO
1063 record 1994/14, 35–42.
- 1064
- 1065 DUDDY, I.R. (1997) Focussing exploration in the Otway Basin: understanding timing of
1066 source rock maturation. *APPEA J.*, 37, 178-191.
- 1067
- 1068 DUDDY, I.R. (2003) Mesozoic, a time of change in tectonic regime. In: *Geology of Victoria*
1069 (Ed. by W.D. Birch), *Geol. Soc. Aust., Spec. Publ.*, 23, 239-286.

- 1070 DUDDY, I.R. & EROUT, B. (2001) AFTA-calibrated 2-D modelling of hydrocarbon
1071 generation and migration using Temispack: preliminary results from the Otway Basin. In:
1072 *Eastern Australian Basins Symposium 2001* (Ed. by K.C. Hill & T. Bernecker), *Petrol. Soc.*
1073 *Aust., Spec. Publ.*, 403–412.
- 1074
- 1075 DUDDY, I.R., EROUT, B., GREEN, P.F., CROWHURST, P.V. & BOULT, P.J. (2003)
1076 Timing constraints on the structural history of the western Otway Basin and implications for
1077 hydrocarbon prospectivity around the Morum High, South Australia. *APPEA J.*, 43, 59-83.
- 1078
- 1079 DYKSTERHUIS, S. & MÜLLER, R.D. (2008) Cause and evolution of intraplate orogeny in
1080 Australia. *Geology*, 36, 495-498.
- 1081
- 1082 EDWARDS J., LEONARD J.G., PETTIFER G.R. & MCDONALD P.A. (1996) Colac 1 :
1083 250 000 map geological report. *Geological Survey of Victoria. Report 98.*
- 1084
- 1085 ETHERIDGE, M., MCQUEEN, H. & LAMBECK, K. (1991) The role of intraplate stress in
1086 Tertiary (and Mesozoic) deformation of the Australian continent and its margins: a key factor
1087 in petroleum trap formation. *Explor. Geophys.*, 22, 123-128.
- 1088
- 1089 GAINA, C., MÜLLER, D.R., ROYER, J-Y., STOCK, J., HARDEBECK, J., & SYMONDS,
1090 P. (1998) The tectonic history of the Tasman Sea: A puzzle with 13 pieces. *J. Geophys. Res.*,
1091 103, 12413-12433.
- 1092
- 1093 GEARY, G.C. & REID, I.S.A. (1998) Geology and prospectivity of the offshore eastern
1094 Otway Basin, Victoria. *Victorian Initiative for Minerals and Petroleum Report*, 55.

- 1095 GIBSON, G.M., MORSE, M.P., IRELAND, T.R. & NAYAK, G.K. (2011) Arc-continent
1096 collision and orogenesis in western Tasmanides: Insights from reactivated basement
1097 structures and formation of an ocean-continent transform boundary off western Tasmania.
1098 *Gond. Res.*, 19, 608-627.
- 1099
- 1100 GIBSON, G.M., TOTTERDELL, J.M., WHITE, L.T., MITCHELL, C.M., STACEY, A.R.,
1101 MORSE, M.P. & WHITAKER, A. (2013) Pre-existing basement structure and its influence
1102 on continental rifting and fracture zone development along Australia's southern rifted margin.
1103 *J. Geol. Soc.*, 170, 365–377.
- 1104
- 1105 GÖLKE, M. & COBLENTZ, D. (1996) Origins of the European regional stress field.
1106 *Tectonophys.*, 266, 11-24.
- 1107
- 1108 GÓMEZ, M. & VERGÉS, J. (2005) Quantifying the contribution of tectonics vs. differential
1109 compaction in the development of domes along the Mid-Norwegian Atlantic margin. *Basin*
1110 *Research*, 17, 289-310.
- 1111
- 1112 GREEN, P.F., CROWHURST, P.V. & DUDDY, I.R. (2004) Integration of AFTA and (U-
1113 Th)/He thermochronology to enhance the resolution and precision of thermal history
1114 reconstruction in the Anglesea-1 well, Otway Basin, SE Australia. In: *Eastern Australian*
1115 *Basins Symposium II* (Ed. by P.J. Boulton, D.R. Johns and S.C. Lang), *Petrol. Explor. Soc.*
1116 *Aust., Spec. Publ.*, 117-131.
- 1117

- 1118 HARROWFIELD, M. & KEEP, M. (2005) Tectonic modification of the Australian North-
1119 West Shelf: episodic rejuvenation of long-lived basin divisions. *Basin Research*, 17, 225–
1120 239.
- 1121
- 1122 HILL, K.C. & HALL, R. (2003) Mesozoic-Cenozoic evolution of Australia's New Guinea margin
1123 in a West Pacific context. In: *Evolution and Dynamics of the Australian Plate* (Ed. by R.R.
1124 Hillis & D. Müller), *Geol. Soc. Aust., Spec. Publ* , 22, 265-290.
- 1125
- 1126 HILL, K.C., HILL, K.A., COOPER, G.T., O'SULLIVAN, A.J., O'SULLIVAN, P.B. &
1127 RICHARDSON, M.J. (1995) Inversion around the Bass Basin, SE Australia. In: *Basin*
1128 *Inversion* (Ed. by J.G. Buchanan & P.G. Buchanan), *Geol. Soc. Spec. Publ.*, 88, 525-547.
- 1129
- 1130 HILLIS, R.R. & REYNOLDS, S.D. (2000) The Australian stress map. *J. Geol. Soc.*, 157,
1131 915–921.
- 1132
- 1133 HILLIS, R.R., MONTE, S.A., TAN, C.P. & WILLOUGHBY, D.R. (1995) The contemporary
1134 stress field of the Otway Basin, South Australia: Implications for hydrocarbon exploration
1135 and production. *APEA J.*, 35, 494-506.
- 1136
- 1137 HILLIS, R.R., HOLFORD, S.P., GREEN, P.F., DORÉ, A.G., GATLIFF. R.W., STOKER,
1138 M.S., THOMSON, K., TURNER, J.P., UNDERHILL, J.R. & WILLIAMS, G.A. (2008a)
1139 Cenozoic exhumation of the southern British Isles. *Geology*, 36, 371-374.
- 1140
- 1141 HILLIS, R.R., SANDIFORD, M., REYNOLDS, S.D. & QUIGLEY, M.C. (2008B) Present-
1142 day stress, seismicity and Neogene-to-Recent tectonics of Australia's 'passive' margins:

- 1143 intraplate deformation controlled by plate boundary forces. In: *The Nature and Origin of*
1144 *Compression in Passive Margins* (Ed. by H. Johnson, A.G. Doré, R.W. Gatliff, R.
1145 Holdsworth, E.R. Lundin, and J.D. Ritchie), *Geol. Soc. Spec. Publ.*, 306, 71-90.
1146
- 1147 HOLDGATE, G. R. & GALLAGHER, S. J. (2003) Tertiary, a period of transition to marine
1148 basin environments. In: *Geology of Victoria* (Ed. by W.D. Birch), *Geol. Soc. Aust., Spec.*
1149 *Publ.*, 23, 289-335.
1150
- 1151 HOLDGATE, G.R., SMITH, T.A.G., GALLAGHER, S.J. & WALLACE, M.W. (2001)
1152 Geology of coal-bearing Palaeogene sediments, onshore Torquay Basin, Victoria. *Aus. J.*
1153 *Earth Sci.*, 48, 657-679.
1154
- 1155 HOLFORD, S.P., GREEN, P.F., TURNER, J.P., WILLIAMS, G.A, HILLIS, R.R., TAPPIN,
1156 D.R. & DUDDY, I.R. (2008) Evidence for km-scale Neogene exhumation driven by
1157 compressional deformation in the Irish Sea basin system. In: *The Nature and Origin of*
1158 *Compression in Passive Margins* (Ed. by H. Johnson, A.G. Doré, R.W. Gatliff, R.
1159 Holdsworth, E.R. Lundin, and J.D. Ritchie), *Geol. Soc. Spec. Publ.*, 306, 91-119..
1160
- 1161 HOLFORD, S.P., GREEN, P.F., DUDDY, I.R., TURNER, J.P., HILLIS, R.R. & STOKER,
1162 M.S. (2009a) Regional intraplate exhumation episodes related to plate boundary deformation.
1163 *Geol. Soc. Am., Bull.*, 121, 1611-1628.
1164
- 1165 HOLFORD S.P., TURNER J.P., GREEN P.F. & HILLIS R.R. (2009b) Signature of cryptic
1166 sedimentary basin inversion revealed by shale compaction data in the Irish Sea, western
1167 British Isles. *Tectonics*, 28, TC4011, doi:10.1029/2008TC002359.

- 1168 HOLFORD, S.P., GREEN, P.F., HILLIS, R.R., UNDERHILL, J.R., STOKER, M.S. &
1169 DUDDY, I.R. (2010a) Multiple post-Caledonian exhumation episodes across northwest
1170 Scotland revealed by apatite fission track analysis. *J. Geol. Soc.*, 167, 675–694.
1171
- 1172 HOLFORD, S.P., HILLIS, R.R., DUDDY, I.R., GREEN, P.F., TUITT, A.K. & STOKER,
1173 M.S. (2010b) Impacts of Neogene-Recent compressional deformation and uplift on
1174 hydrocarbon prospectivity of the 'passive' southern Australian margin. *APPEA J.*, 50, 267-
1175 284.
1176
- 1177 HOLFORD, S.P., HILLIS, R.R., DUDDY, I.R., GREEN, P.F., STOKER, M.S., TUITT,
1178 A.K., BACKE, G., TASSONE, D.R. & MACDONALD, J.D. (2011a) Cenozoic post-breakup
1179 compressional deformation and exhumation of the southern Australian margin. *APPEA J.*, 51,
1180 613-638.
1181
- 1182 HOLFORD, S.P., HILLIS, R.R., DUDDY, I.R., GREEN, P.F., TASSONE, D.R. &
1183 STOKER, M.S. (2011b). Palaeothermal and seismic constraints on late Miocene-Pliocene
1184 uplift and deformation in the Torquay sub-basin, southern Australian margin. *Aust. J. Earth*
1185 *Sci.*, 58, 543-562.
1186
- 1187 HOLFORD, S.P., HILLIS, R.R., HAND, M. & SANDIFORD, M. (2011c) Thermal
1188 weakening localizes intraplate deformation along the southern Australian continental margin.
1189 *Earth Planet. Sci. Lett.*, 305, 217-214
1190
- 1191 HOLFORD, S.P., SCHOFIELD, N., MACDONALD, J.D., DUDDY, I.R. & GREEN, P.F.
1192 (2012) Seismic analysis of igneous systems in sedimentary basins and their impacts on

- 1193 hydrocarbon prospectivity: examples from the southern Australian margin. *APPEA J.*, 52,
1194 229-252.
- 1195
- 1196 HUDEC, M.R. & JACKSON, M.P.A. (2002) Structural segmentation, inversion and salt
1197 tectonics on a passive margin: Evolution of the Inner Kwanza Basin, Angola. *Geol. Soc.*
1198 *Am., Bull.*, 114, 1222-1244.
- 1199
- 1200 JACKSON, C. A.-L. (2012) Seismic reflection imaging and controls on the preservation of
1201 ancient sill-fed magmatic vents. *J. Geol. Soc.*, 169, 503–506.
- 1202
- 1203 JENSEN-SCHMIDT, B., COCKSHELL, C.D. & BOULT, P.J. (2002) Chapter 5: Structural
1204 and tectonic setting. In: *Petroleum Geology of South Australia. Vol. 1: Otway Basin, Second*
1205 *Edition*. (Ed. by P.J. Boulton and J.E. Hibbert).
- 1206
- 1207 JOHNSON, H., DORÉ, A.G., GATLIFF, R.W., HOLDSWORTH, R., LUNDIN, E.R. &
1208 RITCHIE, J.D. (Eds) (2008) *The Nature and Origin of Compression in Passive Margins*,
1209 Special Publications, 306, Geological Society, London.
- 1210
- 1211 KENNETT, B.L.N., SALMON, M., SAYGIN, E. & AUSMOHO WORKING GROUP
1212 (2011) AusMoho: the variation of Moho depth in Australia. *Geophys. J. Int.*, 187, 946-958.
- 1213
- 1214 KING, R., HOLFORD, S., HILLIS, R., TUITT, A., SWIERCZEK, E., BACKÉ, G.,
1215 TASSONE, D. & TINGAY, M (2012) Reassessing the in-situ stress regimes of Australia's
1216 petroleum basins. *APPEA J.*, 52, 415-425.
- 1217

- 1218 KRASSAY, A.A., CATHRO, D.L. & RYAN, D.J. (2004) A regional tectonostratigraphic
1219 framework for the Otway Basin. In: *Eastern Australian Basins Symposium II* (Ed. by P.J.
1220 Boulton, D.R. Johns and S.C. Lang), *Petrol. Explor. Soc. Aust., Spec. Publ.*, 97-106.
1221
- 1222 KRISHNA, K.S., BULL, J.M. & SCRUTTON, R.A. (2001) Evidence for multiphase folding
1223 of the central Indian Ocean lithosphere. *Geology*, 29, 715-718.
1224
- 1225 KULPECZ, A.A., MILLER, K.G., BROWNING, J.V., EDWARDS, L.E., POWARS, D.S.,
1226 MCLAUGHLIN, P.P., JR., HARRIS, A.D. & FEIGENSON, M.D. (2009) Post-impact
1227 deposition in the Chesapeake Bay impact structure: Variations in eustasy, compaction,
1228 sediment supply, and passive-aggressive tectonism. In: *The ICDP-USGS Deep Drilling
1229 Project in the Chesapeake Bay Impact Structure: Results from the Eyreville Core Holes* (Ed.
1230 by G.S. Gohn, C. Koeberl, K.G. Miller, and W.U. Reimold), *Geol. Soc. Am., Spec. Paper*,
1231 458, 811-837.
1232
- 1233 LE BRETON, E., COBBOLD, P.R., DAUTEUIL, O. & LEWIS, G. (2012) Variations in
1234 amount and direction of seafloor spreading along the northeast Atlantic Ocean and resulting
1235 deformation of the continental margin of northwest Europe. *Tectonics*, 31, TC5006,
1236 doi:10.1029/2011TC003087.
1237
- 1238 LEONARD, M. & CLARK, D. (2011) A record of stable continental region earthquakes
1239 from Western Australia spanning the late Pleistocene: Insights for contemporary seismicity.
1240 *Earth Planet. Sci. Lett.*, doi:10.1016/j.epsl.2011.06.035.
1241

- 1242 LI, Q., JAMES, N. P. & MCGOWRAN, B. (2003) Middle and Late Eocene Great Australian
1243 Bight lithostratigraphy and stepwise evolution of the southern Australian continental
1244 margin. *Aust. J. Earth Sci.*, 50, 113-128.
1245
- 1246 LIU, M., STEIN, S. & WANG, H. (2011) 2000 years of migrating earthquakes in North
1247 China: How earthquakes in midcontinents differ from those at plate boundaries. *Lithosphere*,
1248 3, 128-132.
1249
- 1250 LUNDIN, E.R. & DORÉ, A.G. (2002) Mid-Cenozoic post-breakup deformation in the
1251 'passive' margins bordering the Norwegian-Greenland Sea. *Mar. Petr. Geology*, 19, 79-93.
1252
- 1253 LUNDIN, E.R. & DORÉ, A.G. (2011) Hyperextension, serpentinization, and weakening: A
1254 new paradigm for rifted margin compressional deformation. *Geology*, 39, 347-350.
1255
- 1256 MACDONALD, J.D., HOLFORD, S.P., GREEN, P.F., DUDDY, I.R., KING, R.C. &
1257 BACKÉ, G. (2013) Detrital zircon data reveal the origin of Australia's largest delta system. *J.*
1258 *Geol. Soc.*, 170, 3-6.
1259
- 1260 MCCLAY, K.R. (1995) The geometries and kinematics of inverted fault systems: A review
1261 of analogue model studies. In: *Basin Inversion* (Ed. by J.G. Buchanan & P.G. Buchanan),
1262 *Geol. Soc. Spec. Publ.*, 88, 97-118.
1263
- 1264 MCGOWRAN, B., HOLDGATE, G. R., LI, Q. & GALLAGHER, S. J. (2004) Cenozoic
1265 stratigraphic succession in southeastern Australia. *Aust. J. Earth Sci.*, 51, 459-496.
1266

- 1267 MESSENT, B.E., COLLINS, G.I. & WEST, B.G. (1999) Hydrocarbon prospectivity of the
1268 offshore Torquay sub-basin, Victoria: gazettal area V99-1. *Victoria Initiative for Minerals*
1269 *and Petroleum*, 60.
- 1270
- 1271 MILLER, J.McL., NORVICK, M.S. & WILSON, C.J.L. (2002). Basement controls on rifting
1272 and the associated formation of ocean transform faults—Cretaceous continental extension of
1273 the southern margin of Australia. *Tectonophysics*, 359, 131-155.
- 1274 MITCHUM, R. M., VAIL, P. R. & THOMPSON, S. (1977) Seismic stratigraphy and global
1275 changes of sea level, Part 6: stratigraphic interpretation of seismic reflection patterns in
1276 depositional sequences. In: *Seismic Stratigraphy - Applications to Hydrocarbon Exploration*
1277 (Ed. by C.E. Payton), *AAPG Mem.*, 26, 117-133.
- 1278
- 1279 MOSAR, J., LEWIS, G. & TORSVIK, T.H. (2002) North Atlantic sea-floor spreading rates:
1280 implications for the Tertiary development of inversion structures of the Norwegian-
1281 Greenland Sea. *J. Geol. Soc.*, 159, 503-515.
- 1282
- 1283 MÜLLER, R.D., DYKSTERHUIS, S. & REY, P. (2012) Australian paleo-stress fields and
1284 tectonic reactivation over the past 100 Ma. *Aust. J. Earth Sci.*, 59, 13-28.
- 1285
- 1286 NELSON, E.J. & HILLIS, R.R. (2005) In situ stresses of the West Tuna area, Gippsland
1287 Basin. *Austr. J. Earth Sci.*, 52, 299-313.
- 1288
- 1289 NELSON, E.J., HILLIS, R.R., SANDIFORD, M., REYNOLDS, S.D. & MILDREN, S.D.
1290 (2006) Present-day state-of-stress of southeast Australia. *APPEA J.*, 46, 283–305.
- 1291

- 1292 NORVICK, M.S. & SMITH, M.A. (2001) Mapping the plate tectonic reconstruction of
1293 southern and southeastern Australia and implications for petroleum systems. *APPEA J.*, 41,
1294 15–35.
- 1295
- 1296 PASCAL, C., & CLOETINGH, S.A.P.L. (2009) Gravitational potential stresses and stress
1297 field of passive continental margins: Insights from the south-Norway shelf. *Earth Planet. Sci.*
1298 *Lett.*, 277, 464-473.
- 1299
- 1300 PATRIAT, P. & ACHACHE, J. (1984) India–Eurasia collision chronology has implications
1301 for crustal shortening and driving mechanism of plates. *Nature*, 311, 615-621.
- 1302
- 1303 PERINCEK, D. & COCKSHELL, C.D. (1995) The Otway Basin: Early Cretaceous rifting to
1304 Neogene inversion. *APEA J.*, 35, 451–466.
- 1305
- 1306 PERINCEK, D., COCKSHELL, C.D., FINLAYSON, D.M. & HILL, K.A. (1994) The Otway
1307 Basin: Early Cretaceous rifting to Miocene strike-slip. In: *NGMA/PESA Otway Basin*
1308 *Symp.*, (Ed. by D.M. Finlayson), AGSO record 1994/14, 27–33.
- 1309
- 1310 PEREIRA, R., ALVES, T.M. & CARTWRIGHT, J. (2011) Post-rift compression on the SW
1311 Iberian margin (eastern North Atlantic): a case for prolonged inversion in the ocean-continent
1312 transition zone. *J. Geol. Soc.*, 168, 1249-1263.
- 1313
- 1314 PÉRON-PINVIDIC, G., MANATASCHAL, G., DEAN, S.M. & MINSHULL, T.A. (2008)
1315 Compressional structures on the West Iberia rifted margin: controls on their distribution. In:
1316 *The Nature and Origin of Compression in Passive Margins* (Ed. by H. Johnson, A.G. Doré,

- 1317 R.W. Gatliff, R. Holdsworth, E.R. Lundin, and J.D. Ritchie), *Geol. Soc. Spec. Publ.*, 306, 169-
1318 183.
1319
- 1320 POLLOCK, R.M. (2003) *Sequence stratigraphy of the Paleocene to Miocene Gambier Sub-*
1321 *Basin, Southern Australia*. University of Adelaide, Adelaide, Australia.
1322
- 1323 PRAEG, D., STOKER, M.S., SHANON, P.M., CERAMICOLA, S., HJELSTUN, B.O. &
1324 MATHIESEN, A. (2005) Episodic Cenozoic tectonism and the development of the NW
1325 European 'passive' continental margin. *Mar. Pet. Geology*, 22, 1007–1030.
1326
- 1327 QUIGLEY, M., CUPPER, M. & SANDIFORD, M. (2006) Quaternary faults of southern
1328 Australia: palaeoseismicity, slip rates and origin. *Aust. J. Earth Sci.*, 53, 285-301
1329
- 1330 REYNOLDS, S.D., COBLENTZ, D.D. & HILLIS, R.R. (2002) Tectonic forces controlling
1331 the regional intraplate stress field in continental Australia: results from new finite-element
1332 modelling. *J. Geophys. Res.*, 107, B7, doi:10.1029/2001JB000408.
1333
- 1334 REYNOLDS, S.D., COBLENTZ, D.D. & HILLIS, R.R. (2003) Influences of plate-boundary
1335 forces on the regional intraplate stress field of continental Australia. In: *Evolution and*
1336 *Dynamics of the Australian Plate* (Ed. by R.R. Hillis & D. Müller), *Geol. Soc. Aust., Spec.*
1337 *Publ* , 22, 59-70.
1338
- 1339 REYNOLDS, S.D., MILDREN, S.D., HILLIS, R.R. AND MEYER, J.J. (2006) Constraining
1340 stress magnitudes using petroleum exploration data in the Cooper-Eromanga Basins,
1341 Australia. *Tectonophys.*, 415, 123-140.

- 1342 RITCHIE, J.D., JOHNSON, H., QUINN, M.F. & GATLIFF, R.W. (2008) The effects of
1343 Cenozoic compression within the Faroe-Shetland Basin and adjacent areas. In: *The Nature*
1344 *and Origin of Compression in Passive Margins* (Ed. by H. Johnson, A.G. Doré, R.W. Gatliff,
1345 R. Holdsworth, E.R. Lundin, and J.D. Ritchie), *Geol. Soc. Spec. Publ.*, 306, 121-136.
1346
- 1347 SANDIFORD, M. (2003a) Geomorphic constraints on the late Neogene tectonics of the
1348 Otway Range. *Aust. J. Earth Sci.*, 50, 69–80.
1349
- 1350 SANDIFORD, M. (2003b) Neotectonics of south-eastern Australia: linking the Quaternary
1351 faulting record with seismicity and in situ stress. In: *Evolution and Dynamics of the*
1352 *Australian Plate* (Ed. by R.R. Hillis & D. Müller), *Geol. Soc. Aust., Spec. Publ.*, 22, 107–120.
1353
- 1354 SANDIFORD, M. & EGHOLM, D.L. (2008) Enhanced intraplate seismicity across
1355 continental margins: some causes and consequences. *Tectonophysics*, 457, 197-208.
1356
- 1357 SANDIFORD, M. & QUIGLEY, M. (2009) TOPO-OZ: Insights into the various modes of
1358 intraplate deformation in the Australian continent. *Tectonophys.*, 474, 405-416.
1359
- 1360 SANDIFORD, M., WALLACE, M. & COBLENTZ, D. (2004) Origin of the in situ stress
1361 field in southeastern Australia. *Basin Research*, 16, 325–338.
1362
- 1363 SCHNEIDER, C.L., HILL, K.C. & HOFFMAN, N. (2004) Compressional growth of the
1364 Minerva Anticline, Otway Basin, Southeast Australia-evidence of oblique rifting. *APPEA J.*,
1365 44, 463–80.
1366

- 1367 STOKER, M.S., HOULT, R.J., NIELSEN, T., HJELSTUN, B.O., LABERG, J.S.,
1368 SHANNON, P.M., PRAEG, D., MATHIESEN, A., VAN WEERING, T.C.E. &
1369 McDONNELL, A. (2005) Sedimentary and oceanographic responses to early Neogene
1370 compression on the NW European margin. *Mar. Petr. Geology*, 22, 1031-1044.
1371
- 1372 STOKER, M.S., HOLFORD, S.P., HILLIS, R.R., GREEN, P.F. & DUDDY, I.R. (2010)
1373 Cenozoic post-rift sedimentation off NW Britain: recording the detritus of episodic uplift on a
1374 passive continental margin. *Geology*, 39, 595-598.
1375
- 1376 TASSONE, D.R., HOLFORD, S.P., TINGAY, M.R.P., TUITT, A.K., STOKER, M.S. &
1377 HILLIS, R.R. (2011) Overpressures in the central Otway Basin: the result of rapid Pliocene-
1378 Recent sedimentation? *APPEA J.*, 51, 439-458.
1379
- 1380 TASSONE, D.R., HOLFORD, S.P., HILLIS, R.R. & TUITT, A.K. (2012) Quantifying
1381 Neogene plate-boundary controlled uplift and deformation of the southern Australian margin.
1382 In: *Faulting, Fracturing and Igneous Intrusion in the Earth's Crust* (Ed. by D. Healy,
1383 R.W.H. Butler, Z.K. Shipton, and R.H. Sibson), *Geol. Soc. Spec. Publ.*, 367, 91-110.
1384
- 1385 TASSONE, D.R., HOLFORD, S.P., DUDDY, I.R., GREEN, P.F. & HILLIS, R.R. (2013)
1386 Quantifying Cretaceous-Cenozoic exhumation in the Otway Basin using sonic velocity data:
1387 implications for conventional and unconventional hydrocarbon prospectivity. *AAPG Bull.*,
1388 doi:10.1306/04011312111
1389
- 1390 TICKELL S. J., EDWARDS J. & ABELE C. (1992) Port Campbell Embayment 1:100 000
1391 map geological report (and map). *Geological Survey of Victoria Report 95.*

- 1392 TOTTERDELL, J. (2012) New exploration opportunities along Australia's southern margin.
1393 *APPEA J.*, 51, 439-458.
1394
- 1395 TOWNEND, J. & ZOBACK, M.D. (2000) How faulting keeps the crust strong. *Geology*, 28,
1396 399-402.
1397
- 1398 TRUPP, M.A., SPENCE, K.W. & GIDDING, M.J. (1994) Hydrocarbon prospectivity of the
1399 Torquay Sub-Basin, Offshore Victoria. *APEA J.*, 34, 479-494.
1400
- 1401 TUITT, A., UNDERHILL, J.R., RITCHIE, J.D., JOHNSON, H. & HITCHEN, K. (2010)
1402 Timing, controls and consequences of compression in the Rockall-Faroe area of the NE
1403 Atlantic Margin. In: *Proceedings of the 7th Petroleum Geology Conference: From mature*
1404 *basins to new frontiers* (Ed. by B.A. Vining & S. Pickering), pp. 963-977. The Geological
1405 Society, London.
1406
- 1407 TURNER, J.P. & WILLIAMS, G.D. (2004) Sedimentary basin inversion and intra-plate
1408 shortening. *Earth Sci. Reviews* 65, 277-304.
1409
- 1410 TURNER, J.P., GREEN, P.F., HOLFORD, S.P. & LAWRENCE, S.R. (2008) Thermal
1411 history of the Rio Muni (West Africa)-NE Brazil margins during continental breakup. *Earth*
1412 *Planet. Sci. Lett.*, 270, 354-367.
1413
- 1414 VÅGNES, E., GABRIELSEN, R.H. & HAREMO, P. (1998) Late Cretaceous-Cenozoic
1415 intraplate contractional deformation at the Norwegian continental shelf: timing, magnitude
1416 and regional implications. *Tectonophys.* 300, 29-46.

- 1417 VÁZQUEZ, J.T., MEDIALDEA, T., ERCILLA, G., SOMOZA, L., ESTRADA, F.,
1418 FERNÁNDEZ PUGA, M.C., GALLART, J., GRÀCIA, E., MAESTRO, A. & SAYAGO, M.
1419 (2008) Cenozoic deformational structures on the Galicia Bank Region (NW Iberian
1420 continental margin). *Mar. Geology*, 249, 128–149.
- 1421
- 1422 VEEVERS, J.J. (2000) Change of tectono-stratigraphic regime in the Australian plate during
1423 the 99 Ma (mid-Cretaceous) and 43 Ma (mid-Eocene) swerves of the Pacific. *Geology*, 28,
1424 47-50.
- 1425
- 1426 WESSEL, P. & KROENKE, L.W. (2000) Ontong Java Plateau and late Neogene changes in
1427 Pacific plate motion. *J. Geophys. Res.*, 105, 28255–28277.
- 1428
- 1429 WILLIAMS, G.D., POWELL, C.M. & COOPER, M.A. (1989) Geometry and kinematics of
1430 inversion tectonics. In: *Inversion Tectonics* (Ed. by M.A. Cooper & G.D. Williams), *Geol.*
1431 *Soc. Spec. Publ.*, 44, 3-15.
- 1432
- 1433 WILLIAMS, G.A., TURNER, J.P. & HOLFORD, S.P. (2005) Inversion and exhumation of
1434 the St George's Channel Basin, offshore Wales, UK. *J. Geol. Soc.*, 162, 97-110.
- 1435
- 1436 WILLIAMS, S.E., WHITTAKER, J.M. & MÜLLER, R.D. (2011) Full-fit, palinspastic
1437 reconstruction of the conjugate Australian-Antarctic margins. *Tectonics*, 30, TC6012,
1438 doi:10.1029/2011TC002912.
- 1439
- 1440 ZIEGLER, P.A., CLOETINGH, S. & VAN WEES, J.D. (1995) Dynamics of intra-plate

1441 compressional deformation: the Alpine foreland and other examples. *Tectonophys.*, 252, 7-
1442 59.

1443

1444 ZOBACK, M.L. & ZOBACK, M. (2007) Lithosphere Stress and Deformation. In: *Treatise*
1445 *on Geophysics* (Ed. by G. Schubert), 6, 253-273.

1446

1447 **FIGURE CAPTIONS**

1448 **Figure 1.** Indo-Australian plate boundaries and associated forces, and state of stress within
1449 the Australian continent (modified after Reynolds *et al.*, 2002). Large black arrows indicate
1450 mid-ocean ridge driving forces, small black arrows indicate resisting forces associated with
1451 continental collisions and subduction zones, white arrows indicate buoyancy forces resulting
1452 from lithospheric density variations, grey arrows indicate mean maximum horizontal stress
1453 orientations within the Australian continent (length of bars is proportional to data quality).

1454 H, Himalaya; S, Sumatra Trench; J, Java Trench; B, Banda Arc; NG, New Guinea; SM,
1455 Solomon Trench; NH, New Hebrides; LHR, Lord Howe Rise; TK, Tonga-Kermadec Trench;
1456 NZ, New Zealand; SNZ, south of New Zealand; MOR, mid-ocean ridge; cb, collisional
1457 boundary; sz, subduction zone; is, island arc.

1458

1459 **Figure 2. A.** Otway Basin location map. Inset map shows 2D seismic lines used to map
1460 Cenozoic unconformities and compressional structures. Northern limit of Cenozoic marine
1461 deposits, Lower Cretaceous inliers and major extensional structures modified from Krassay *et*
1462 *al.* (2004). Location/structural element acronyms: COB, continent-ocean boundary; MH,
1463 Merino High; MFZ, Mussel Fault Zone; MSB, Morum sub-basin; NSB, Nelson sub-basin;
1464 OR, Otway Ranges; PO, Portland Trough; PT, Penola Trough; SF, Sorell Fault; ST,
1465 Shipwreck Trough; TFZ, Tartwaup Fault Zone; TSB, Torquay sub-basin. Well acronyms:

1466 A1, Argonaut-1; AS1, Anglesea-1; BB1, Bridgewater Bay-1; BR1, Breaksea Reef-1; CH1,
1467 Chama-1A; CM1, Champion-1; CO1, Copa-1; CR1, Crayfish-A1; D1, Digby-1; DB1,
1468 Discovery Bay-1; ER1, Eric the Red-1; HC1, Hindhaugh Creek-1; LA1, Loch Ard-1; LB1,
1469 La Bella-1; MI1, Minerva-1; MO1, Morum-1; MU1, Mussel-1; NA1, Nautilus-1; NE1,
1470 Neptune-1; NO1, Normanby-1; NP1, Neptune-1; PE1, Pecten-1; TI1, Triton-1; TO1, Troas-1;
1471 TR1, Trumpet-1; V1, Voluta-1. **B.** Western Otway Basin location map, showing positions of
1472 seismic lines displayed in Figures 6-9, and hydrocarbon fields in the western Otway Basin.
1473 Cenozoic structural elements based on this study and Perineck & Cockshell (1995). A, B and
1474 C refer to structural components of the Copa Anticline. **C.** Eastern Otway Basin location
1475 map, showing positions of seismic lines and cross sections displayed in Figures 10-14, and
1476 onshore and offshore hydrocarbon fields in the Port Campbell Embayment and Shipwreck
1477 Trough. Cenozoic structural elements based on this study, Geary & Reid (1998) and Clark *et*
1478 *al.* (2011). Cenozoic structural element acronyms: BF, Bambra Fault; CCF, Castle Cove
1479 Fault; CM, Curdie Monocline; DEM, Devil's Elbow Monocline; Ferguson Hill Anticline,
1480 FHA; Johanna Fault. Acronyms of wells not given in Figure 2A: BC1, Barton Corner-1; FH1,
1481 Fergusons Hill-1; NP3, North Paaratte-3; PC4, Port Campbell-4; R1, Rowans-1; S1,
1482 Seaview-1. **D.** Tectonic elements map for southeastern Australia, showing major basement
1483 terranes and structures and location of the continent-ocean boundary (modified after Gibson
1484 *et al.*, 2011) and the depth to the seismological Moho (modified after Kennett *et al.*, 2011).
1485
1486 **Figure 3.** Stratigraphic chart for the Otway Basin (modified after Krassay *et al.*, 2004).
1487 Acronyms of regional unconformities used in seismic mapping: MPU, late Miocene-Pliocene
1488 unconformity; IOU, intra-Oligocene unconformity; ILU, intra-Lutetian unconformity; IMU,
1489 intra-Maastrichtian unconformity; MCU, mid-Cretaceous unconformity.
1490

1491 **Figure 4.** Lithostratigraphic well correlation from Morum-1 in the northwest part of the
1492 Otway Basin to Eric the Red-1 in the southeast, demonstrating variations in thickness of the
1493 unconformity-bound Cenozoic Wangerrip, Nirranda and Heytesbury Groups (colour schemes
1494 and acronyms are the same as those used in Figure 3). The thickness of the Cenozoic
1495 succession is generally less than 1 km, with pronounced thinning across the Morum-Copa and
1496 Loch Ard structural highs. Thick localised post-MPU successions in the basin centre
1497 represent Pliocene-Recent marine clastic sediments deposited in submarine canyons (Tassone
1498 *et al.*, 2011). Distance between wells is not to scale. Formation tops picked using well
1499 completion reports and PGS' SAMDA (Southern Australian Margin Digital Atlas) database.

1500

1501 **Figure 5.** Time-structure maps (in seconds (s) two-way travel-time) based on regional
1502 seismic mapping of the **A.** intra-Oligocene, **B.** intra-Lutetian, and **C.** intra-Maastrichtian
1503 unconformities.

1504

1505 **Figure 6. A.** Uninterpreted and **B.** interpreted seismic profile 85-02, perpendicular to the fold
1506 axis of the Morum Anticline. Folding of the IMU and ILU is most likely related to reverse-
1507 slip along underlying reactivated Cretaceous normal faults, though these faults still exhibit
1508 net-normal displacements. Thermal history data from the Morum-1, which indicate
1509 substantial mid-Eocene erosion at the ILU are presented in Figure 17A. Seismic profile
1510 provided by PGS.

1511

1512 **Figure 7. A.** Uninterpreted and **B.** interpreted seismic profile 85-13, parallel to the fold axis
1513 of the Morum Anticline. Interpretation modified after Duddy *et al.* (2003). Seismic profile
1514 provided by PGS.

1515

1516 **Figure 8. A.** Uninterpreted and **B.** interpreted seismic profile CO88-11, perpendicular to the
1517 fold axis of the Copa A anticline. Seismic profile provided by PGS.

1518

1519 **Figure 8. A.** Uninterpreted and **B.** interpreted seismic profile CO88-11, perpendicular to the
1520 fold axis of the Copa A anticline. Folding of the IMU and ILU is most likely related to
1521 reverse-slip along underlying reactivated Cretaceous normal faults, though these faults still
1522 exhibit net-normal displacements. Seismic profile provided by PGS.

1523

1524 **Figure 9. A.** Uninterpreted and **B.** interpreted seismic profile CO88-22, perpendicular to the
1525 fold axis of the Copa B anticline. Seismic profile provided by PGS.

1526

1527 **Figure 10. A.** Uninterpreted and **B.** interpreted seismic profile OH91-113, perpendicular to
1528 the fold axis of the low-amplitude Pecten Anticline, which correlates with the onshore Curdie
1529 Monocline. Black arrows indicate erosional truncation of strata beneath the MPU. Further
1530 low-amplitude folding of Cenozoic sediments towards the SSE section of the profile is
1531 associated with the Minerva, Point Ronald and Crowes anticlines. Seismic profile provided
1532 by DPI Victoria.

1533

1534 **Figure 11.** Onshore NW-SE cross-section from the Port Campbell Embayment to Otway
1535 Ranges, modified after Edwards *et al.* (1996). It is suggested here that the Curdie Monocline,
1536 Ferguson Hill Anticline and Crowes Anticline correlate with offshore Cenozoic folds of
1537 similar trends (the Pecten, Minerva and Crowes Anticlines, respectively). Note that this
1538 interpretation shows (often substantial) net-reverse slip along the shallow segments of many
1539 of the normal faults that controlled deposition of the Cretaceous section. Similar evidence for
1540 net-reverse displacement on faults imaged on offshore seismic sections is lacking, but this

1541 may reflect increasing intensity of deformation from the SW to NE in the eastern Otway
1542 Basin, consistent with the marked increase in onshore topography towards the Otway Ranges.

1543

1544 **Figure 12. A.** Uninterpreted and **B.** interpreted seismic profile OE80A-1056, parallel to the
1545 fold axis of the Minerva Anticline. Thermal history data from the Minerva-1 well are
1546 presented in Figure 17C. Small black arrows indicate onlap of late Oligocene-early Miocene
1547 sediments onto the crest of the Minerva Anticline. Seismic profile provided by PGS.

1548

1549 **Figure 13. A.** Uninterpreted and **B.** interpreted seismic profile OE81-2011, perpendicular to
1550 the fold axis of the Point Ronald Anticline. Whilst it is possible to interpret key
1551 unconformities, poor seismic quality within the Cretaceous section makes identification of
1552 faults difficult. This fold is tentatively interpreted as being caused by reverse-reactivation of
1553 an E-dipping Cretaceous normal fault. Seismic profile provided by PGS.

1554

1555 **Figure 14. A.** Uninterpreted and **B.** interpreted seismic profile OH91-210, perpendicular to
1556 the fold axes of the Crowes (left) and Loch Ard (right) anticlines. Seismic profile provided by
1557 DPI Victoria.

1558

1559 **Figure 15.** Compilation map showing Cenozoic structures in the Otway Basin (based on this
1560 study, Perineck & Cockshell (1995) and Clark *et al.*, (2011)) and present-day maximum
1561 horizontal stress orientations determined for a number of onshore and offshore hydrocarbon
1562 exploration wells and boreholes (modified after Nelson *et al.*, 2006). Wherever possible,
1563 structures have been coded to denote the broad period of time during which their post-
1564 breakup activity initiated. Note that it is difficult to demonstrate the pre-late Miocene
1565 deformation histories of many of the onshore structures shown on this map, and it is possible

1566 that some of these structures also record earlier deformation. Structures broadly trend ~NE-
1567 SW irrespective of the timing of their initiation. These orientations are approximately
1568 orthogonal to the ~NW-SE present-day maximum horizontal stress orientation. The focal
1569 mechanism for the December 2nd 1977 $M_L = 4.4$ Balliang earthquake is also shown (after
1570 Denham *et al.*, 1981). The focal mechanism is considered to be poorly constrained but
1571 nonetheless indicates thrust faulting due to ~NW-SE-directed compression, consistent with
1572 present-day stress measurements and geological evidence from this area.

1573

1574 **Figure 16.** Chronology of post-breakup deformation in the Otway Basin, in relation to
1575 regional stratigraphy (after Holdgate & Gallagher, 2003) and plate boundary events that
1576 likely influenced the local stress field. Vertical black bars indicate approximate extent of
1577 activity of individual structures, based on seismic mapping, stratigraphic evidence and
1578 previous studies as described in the text. Vertical white boxes represent estimates of the time
1579 intervals during which Cenozoic and/or Cretaceous sedimentary sections began to cool from
1580 palaeotemperature peaks based on AFTA data from exploration wells. In most cases the
1581 cooling can be attributed to exhumation which accompanied compressional growth of the
1582 structures into which wells have been drilled. Post-late Miocene approximate slip rates are
1583 indicated for selected onshore faults, after Clark *et al.* (2011). Horizontal grey bars represent
1584 time ranges of the unconformities used in seismic mapping. Sources of information used to
1585 compile the plate boundary events are as follows: Southern Ocean half-spreading rates (Li *et*
1586 *al.*, 2004); timing of breakup off the Otway Basin and onset of fast-spreading (Norvick &
1587 Smith, 2001); Wharton Basin Ridge spreading cessation (Dyksterhuis & Müller, 2008);
1588 Tasman Sea spreading cessation (Gaina *et al.*, 1998); orogenic events (Dickinson *et al.*,
1589 2002). Stratigraphic acronyms: BG, Brighton Group; DBG, Demons Bluff Group; EVG,

1590 Eastern View Group; HG, Heytesbury Group; NG, Nirranda Group; TG, Torquay Group;
1591 WG, Wangerrip Group.

1592

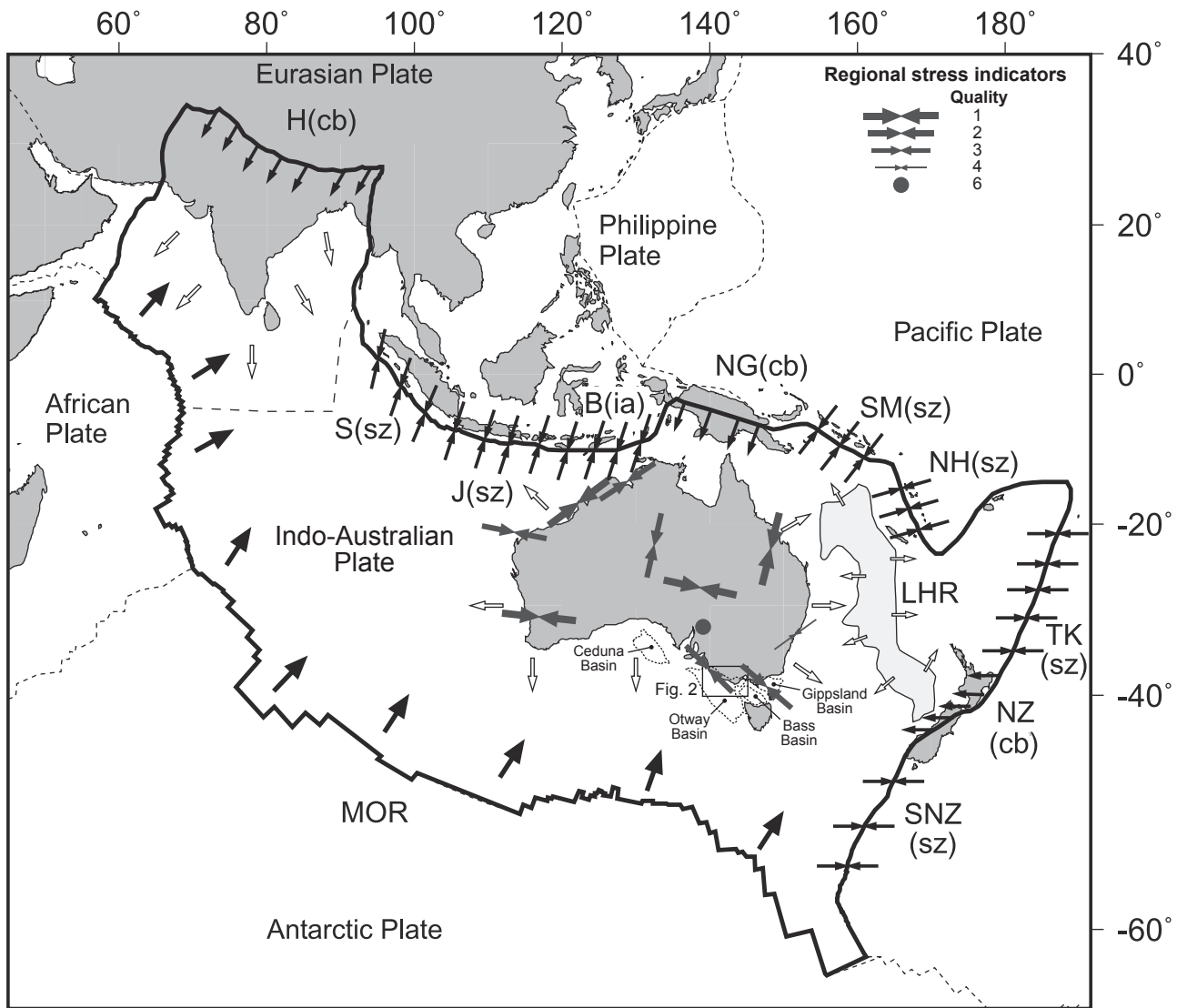
1593 **Figure 17. A.** (Left) Palaeotemperatures derived from AFTA, VR and apatite (U-Th)/He data
1594 from the Morum-1 well plotted against depth and the estimated present-day geothermal
1595 gradient. Integration of these data suggests that Cretaceous section began to cool from
1596 palaeotemperatures that were significantly higher than present-day temperatures between 57
1597 and 40 Ma. Similarity between the gradients of the present-day and palaeotemperature
1598 profiles indicates that cooling was caused by exhumation. Full details of thermal history data
1599 and their interpretation are provided by Duddy *et al.* (2003). (Right) Ranges of amounts of
1600 section removed from the top-Sherbrook Group unconformity (ILU) and palaeogeothermal
1601 gradients (hyperbolic ellipsoid) required to explain the palaeotemperatures estimated from
1602 AFTA, apatite (U-Th)/He and VR data. The hyperbolic ellipsoid defines the parameter ranges
1603 that are consistent with the palaeotemperature constraints within 95% confidence limits. The
1604 black dot indicates maximum likelihood solution values of palaeogeothermal gradient and
1605 removed section. For a mid-Eocene palaeogeothermal gradient equal to the present-day
1606 geothermal gradient of $29.2^{\circ}\text{C km}^{-1}$, 1500 m of section removed at the top Sherbrook Group
1607 unconformity (ILU) is allowed by the data. **B.** (Left) Palaeotemperatures derived from
1608 AFTA, VR and apatite (U-Th)/He data from the Nerita-1 well plotted against depth and the
1609 estimated present-day geothermal gradient. These data indicate that the drilled section has
1610 been considerably hotter in the past, and coupled modelling of AFTA and apatite (U-Th)/He
1611 data suggest that the Cretaceous-Cenozoic section began to cool from these elevated
1612 palaeotemperatures between 10 and 3 Ma. Full details of thermal history data and their
1613 interpretation are provided by Holford *et al.* (2011b). (Right) Ranges of amounts of section
1614 removed from the top-Torquay Group unconformity (MPU) and palaeogeothermal gradients

1615 (hyperbolic ellipsoid) required to explain the palaeotemperatures estimated from AFTA,
1616 apatite (U-Th)/He and VR data. For a palaeogeothermal gradient of $31.5^{\circ}\text{C km}^{-1}$, equal to the
1617 present-day gradient, approximately 1100 m of removed section is required on the top-
1618 Torquay Group unconformity in order to honour the palaeotemperature constraints. **C.** (Left)
1619 Palaeotemperatures derived from AFTA and VR data from the Minerva-1 well plotted against
1620 depth and the estimated present-day geothermal gradient. Similarity between the present-day
1621 and palaeotemperature estimates suggests that the Cenozoic-Cretaceous section drilled by this
1622 well is currently at maximum post-depositional palaeotemperatures. Full details of thermal
1623 history data and their interpretation are provided by Holford *et al.* (2010). (Right) Ranges of
1624 amounts of allowed section removed from the top-Heytesbury Group unconformity (MPU)
1625 and palaeogeothermal gradients (hyperbolic ellipsoid) required to explain the
1626 palaeotemperatures estimated from AFTA and VR data. For a palaeogeothermal gradient of
1627 $42.2^{\circ}\text{C km}^{-1}$, equal to the value of the present-day gradient, no section is required to be
1628 removed from the top-Heytesbury Group unconformity to honour constraints from AFTA and
1629 VR. About 350 m of erosion is allowed by the data, assuming that the geothermal gradient
1630 has increased over time from $35^{\circ}\text{C km}^{-1}$ at the time of erosion to the present-day value.

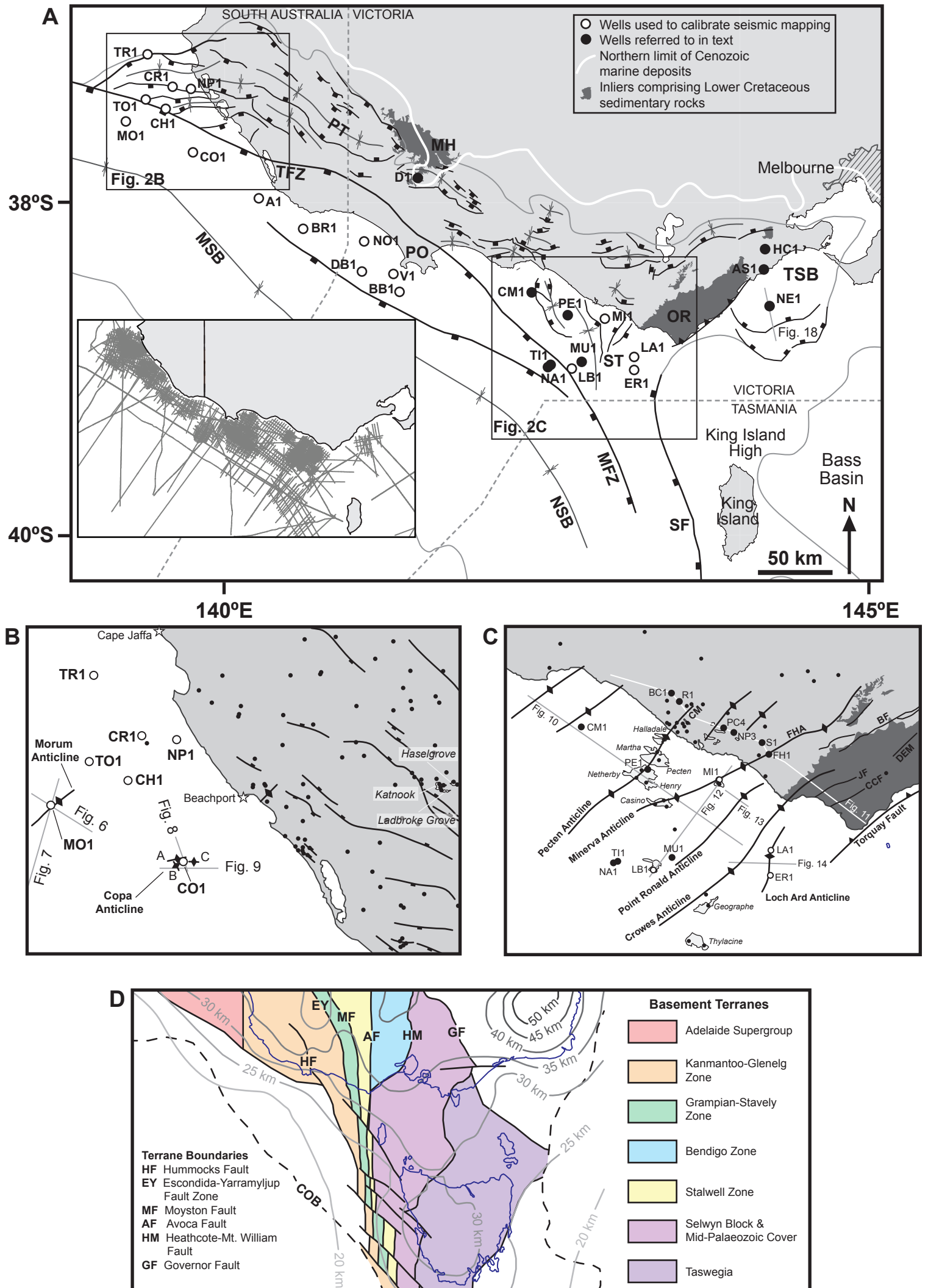
1631

1632 **Figure 18. A.** Uninterpreted and **B.** interpreted seismic profile O40-21, perpendicular to the
1633 fold axes of the Nerita Anticline in the Torquay sub-basin. Thermal history data from the
1634 Nerita-1 well are presented in Figure 17B. Seismic profile provided by PGS.

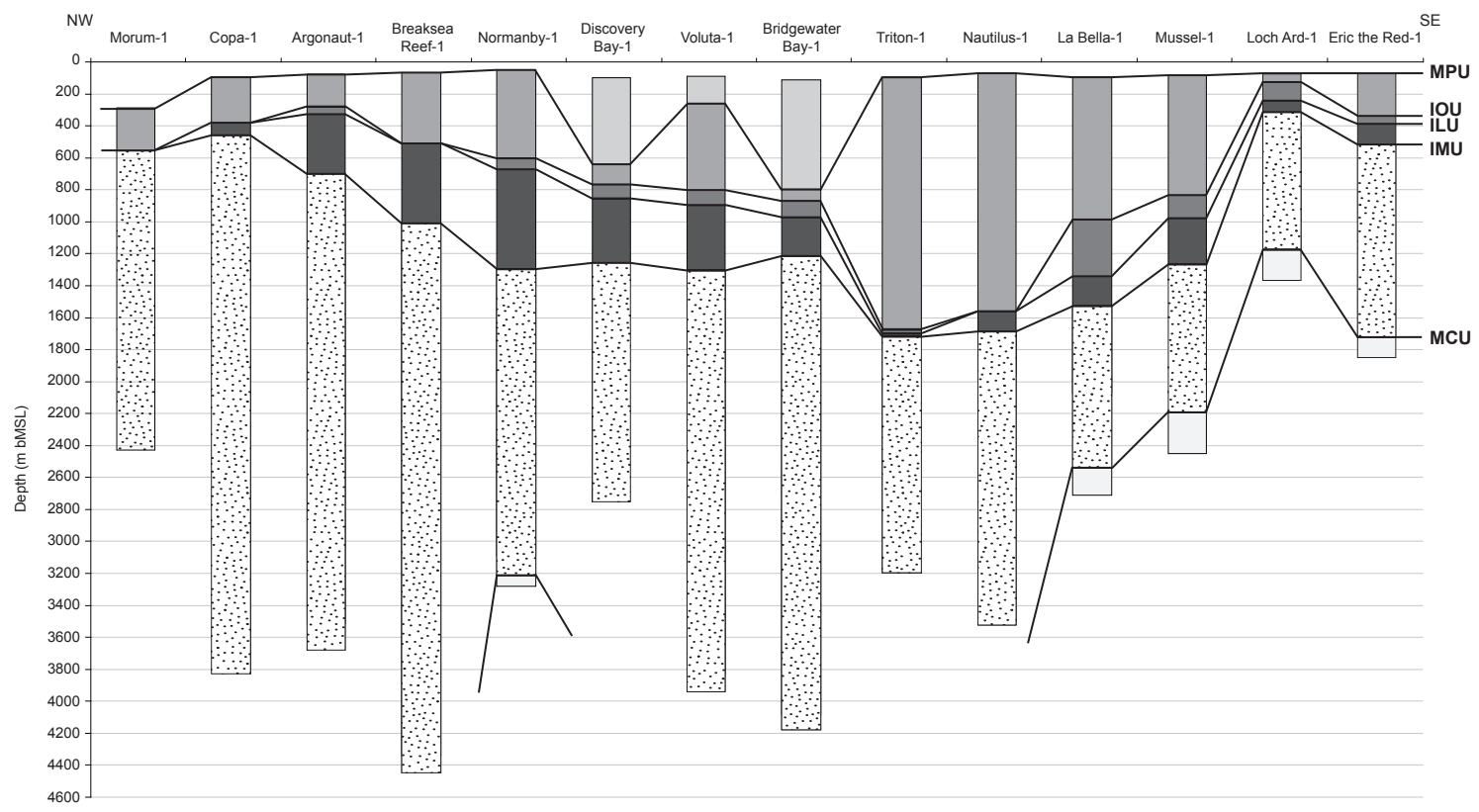
Holford et al Figure 1



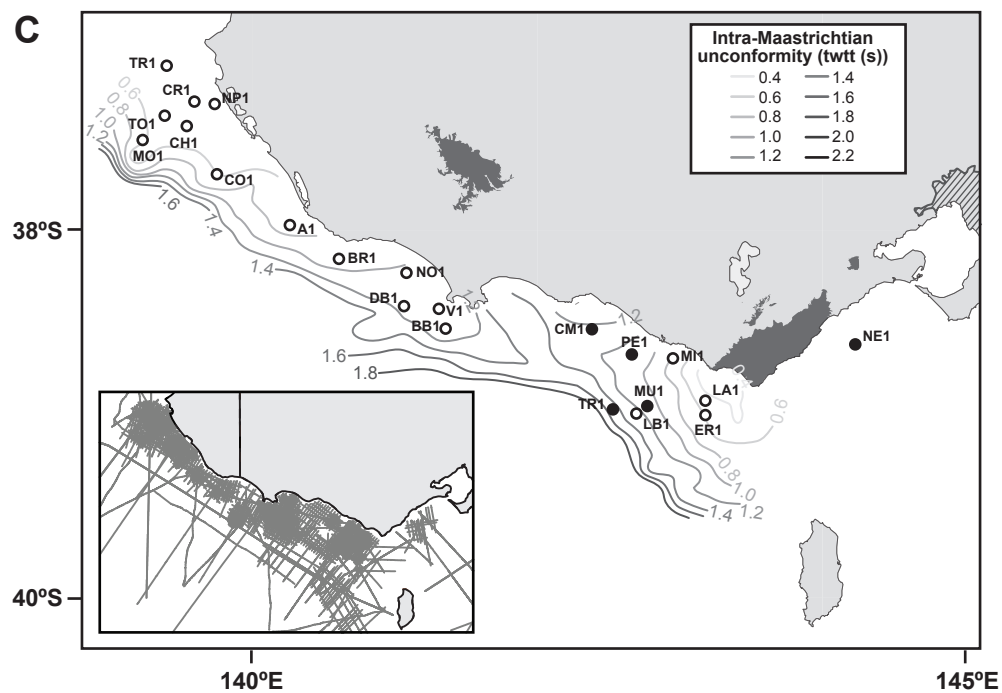
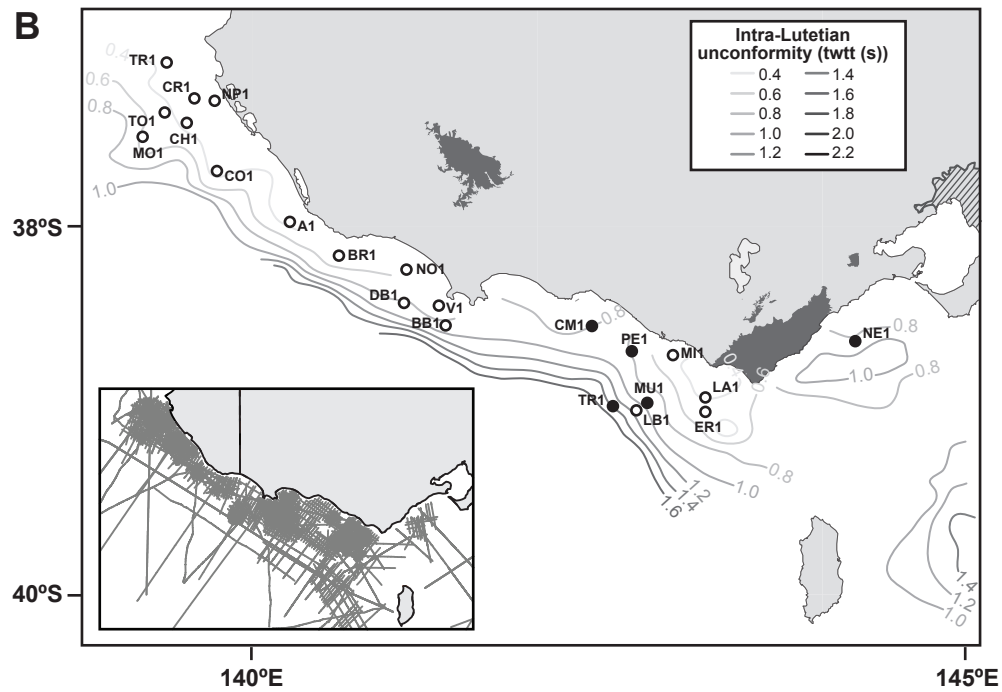
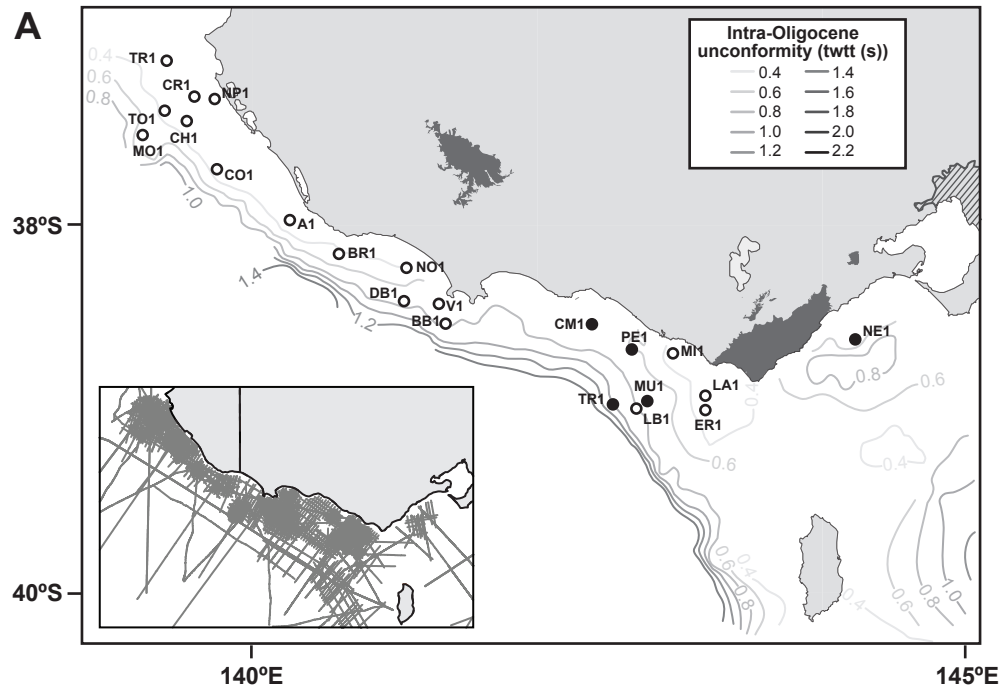
Holford et al Figure 2



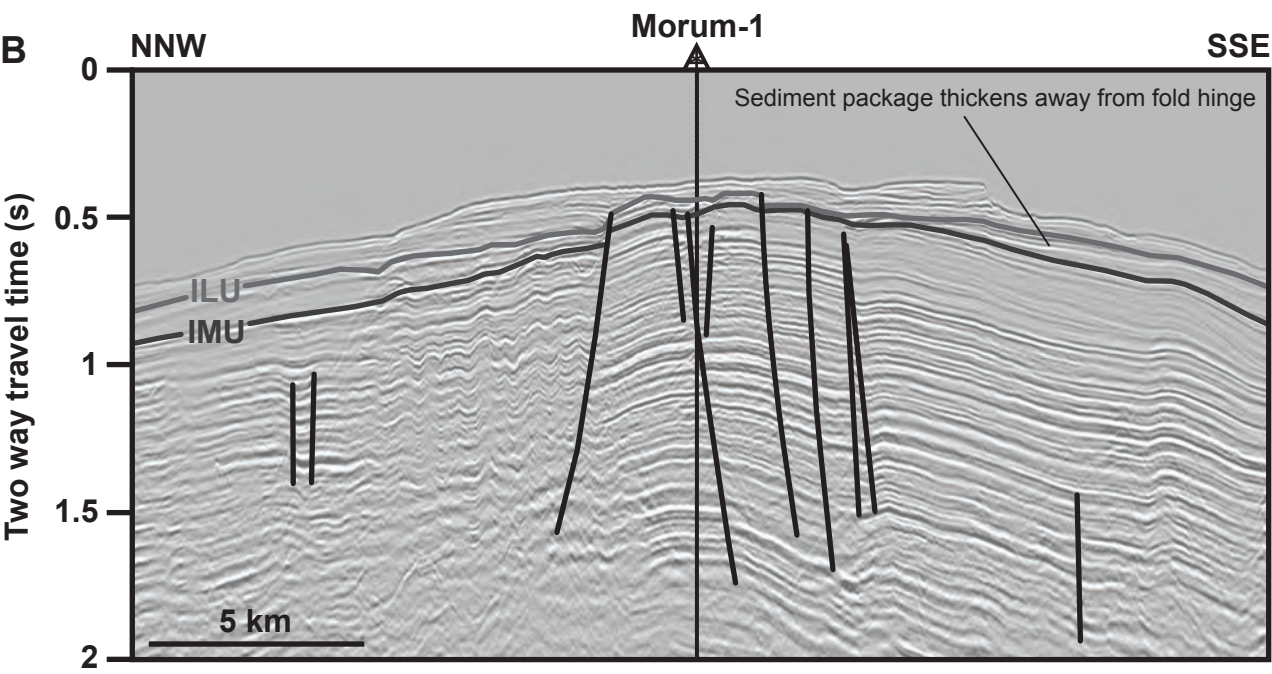
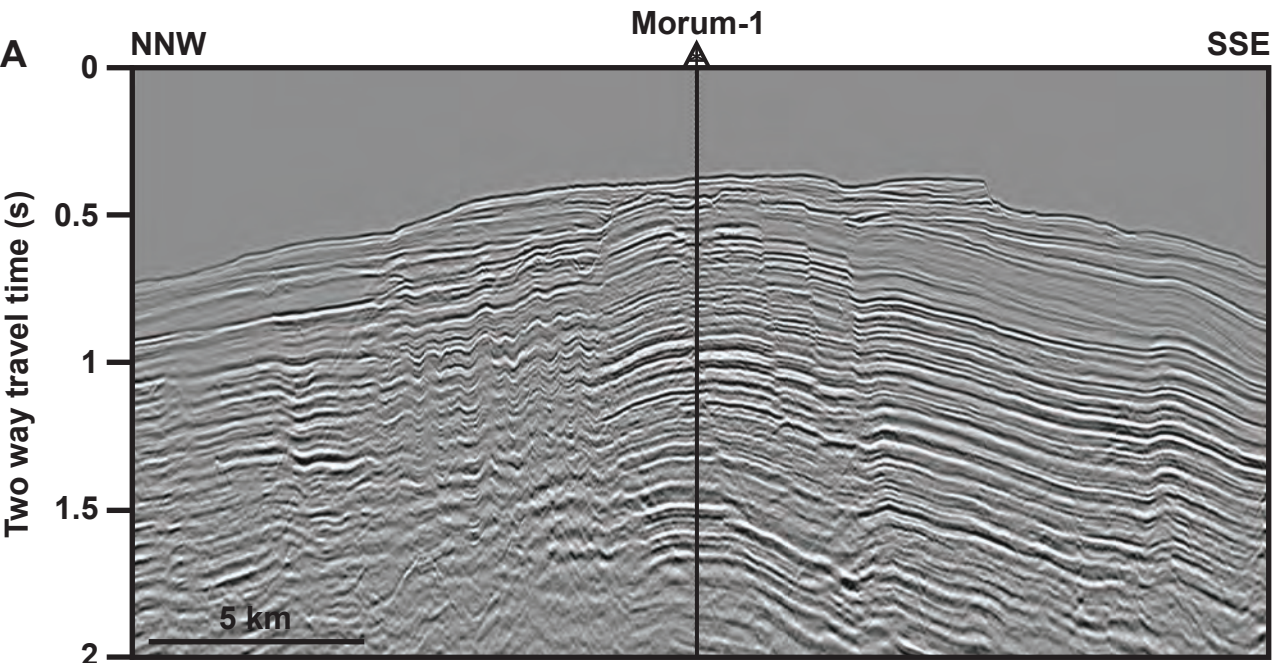
Holford et al Figure 4



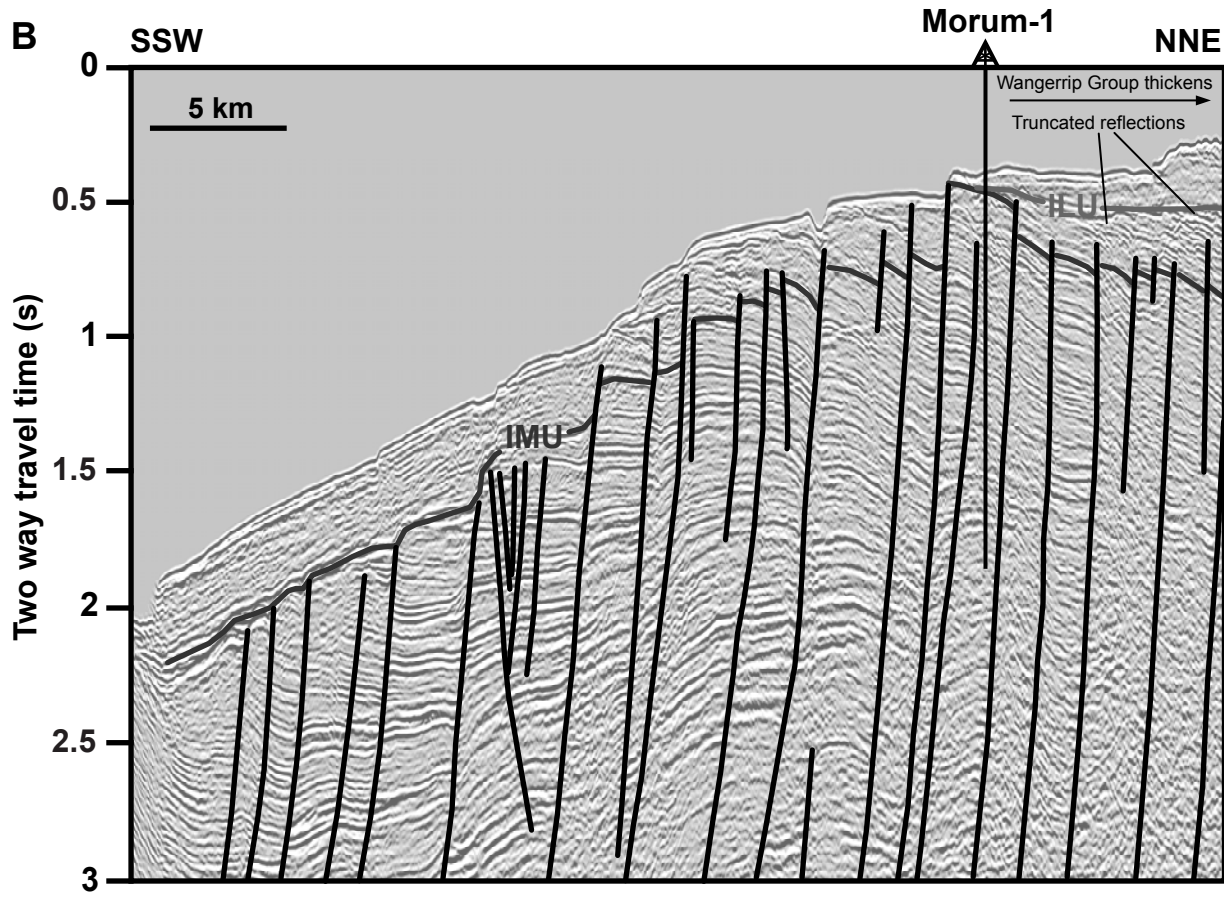
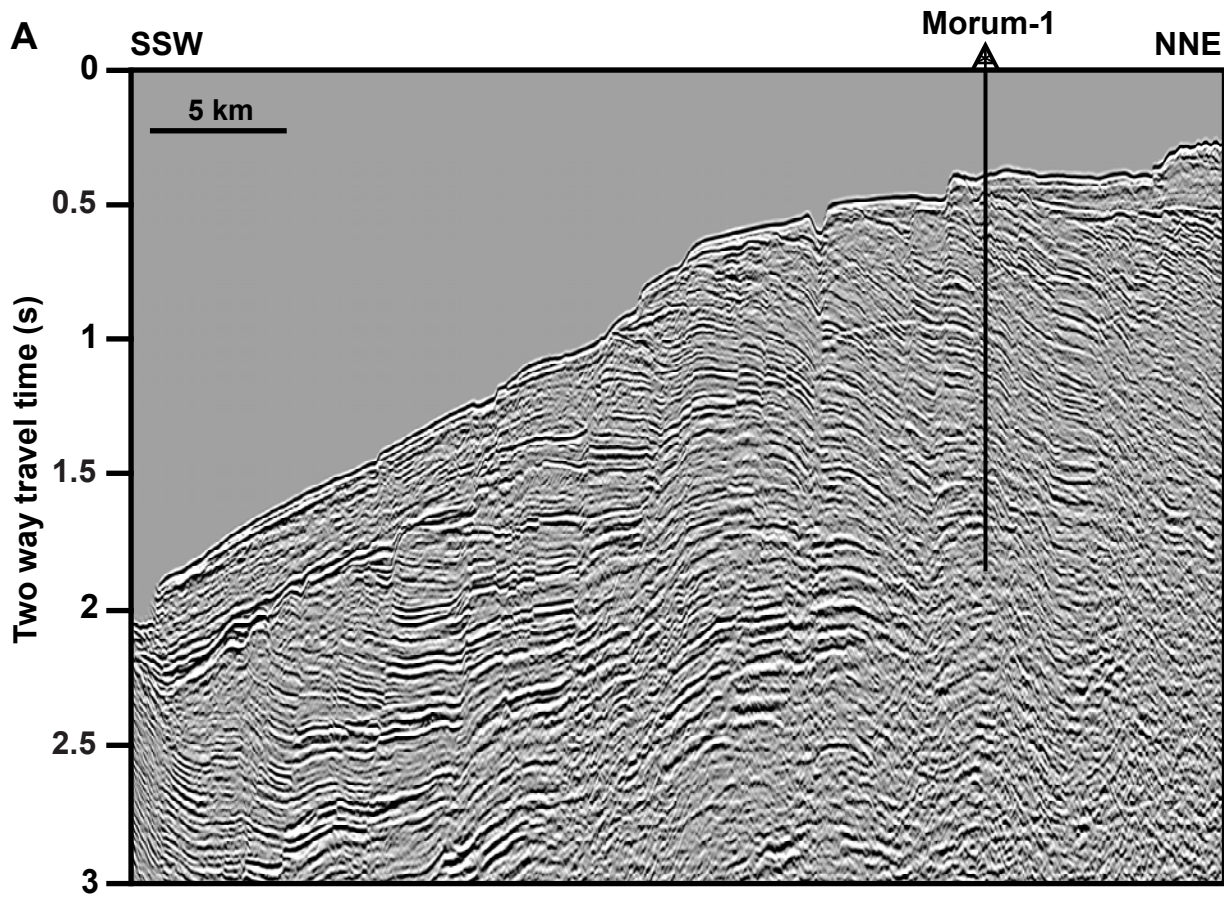
Holford et al Figure 5



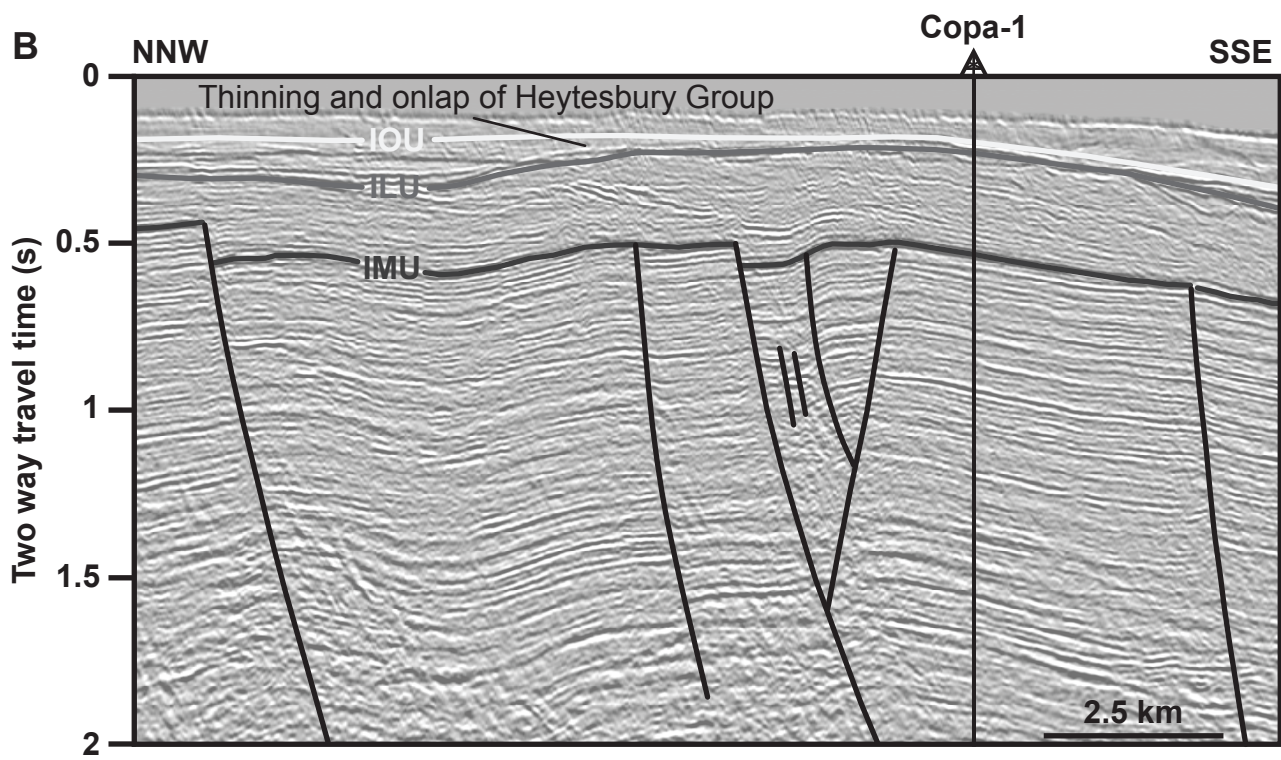
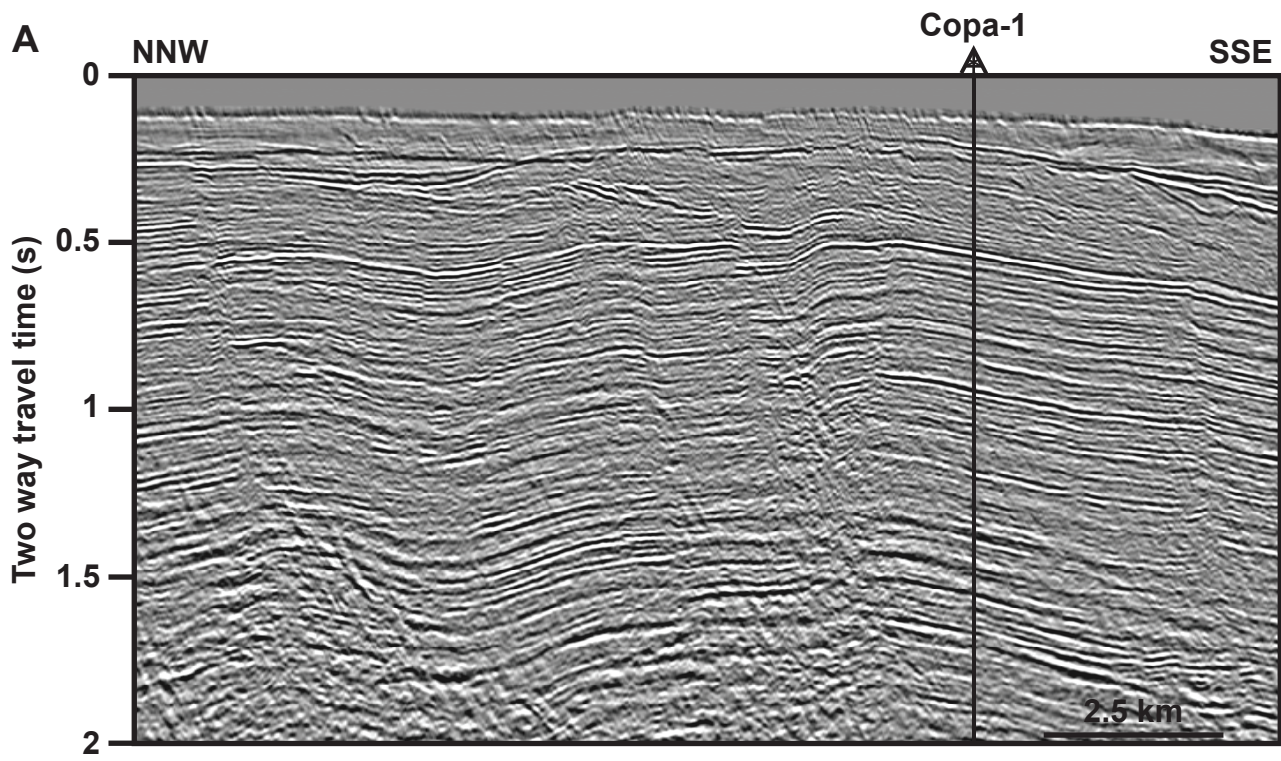
Holford et al Figure 6



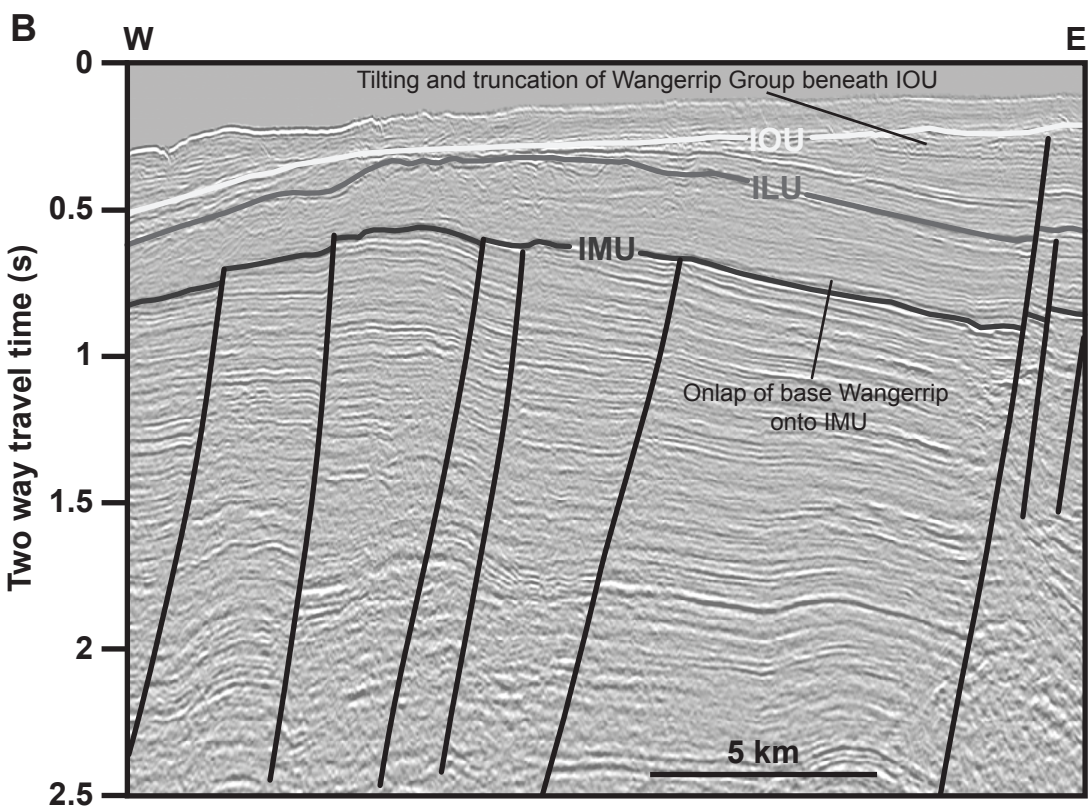
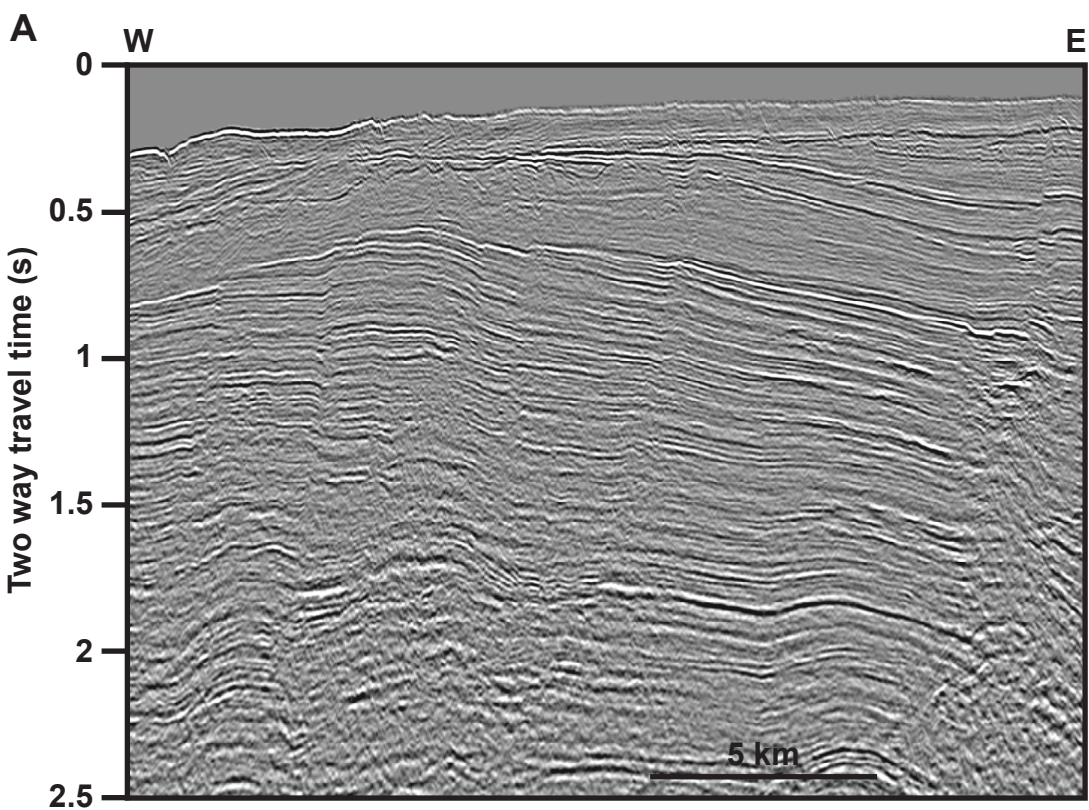
Holford et al Figure 7

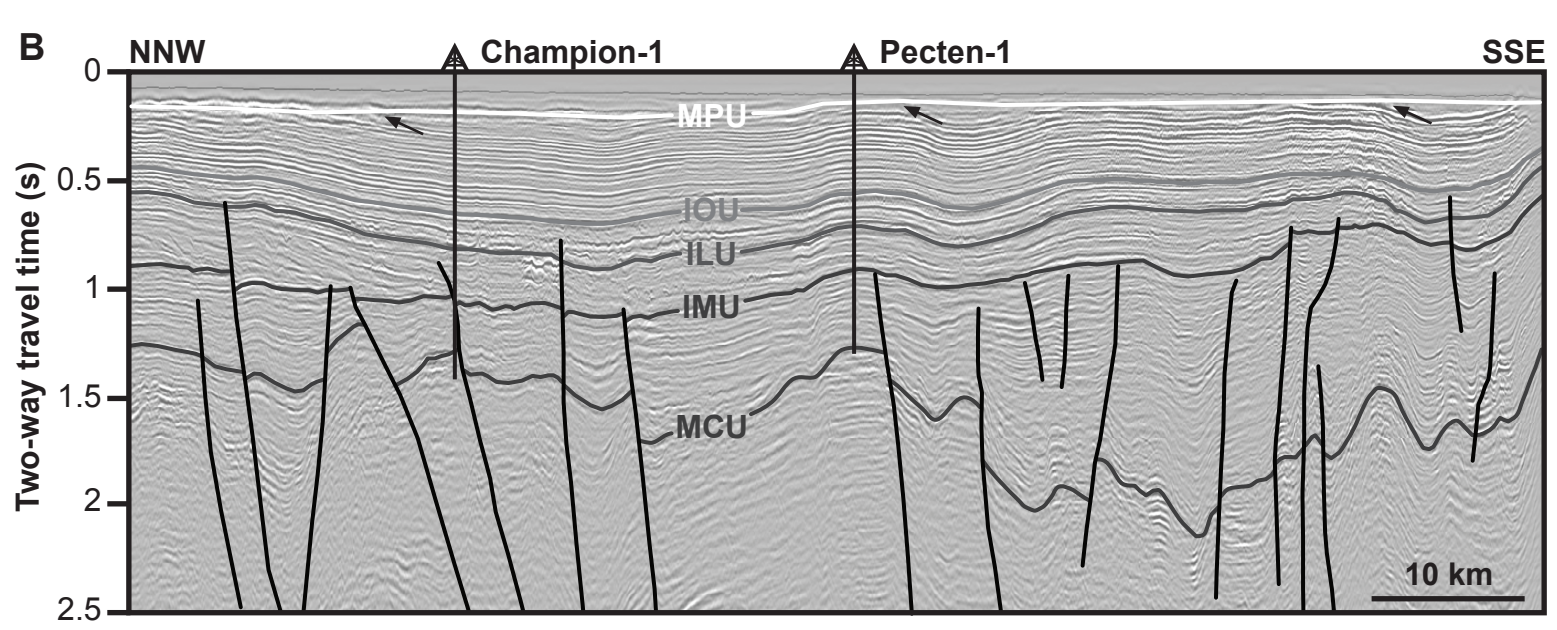
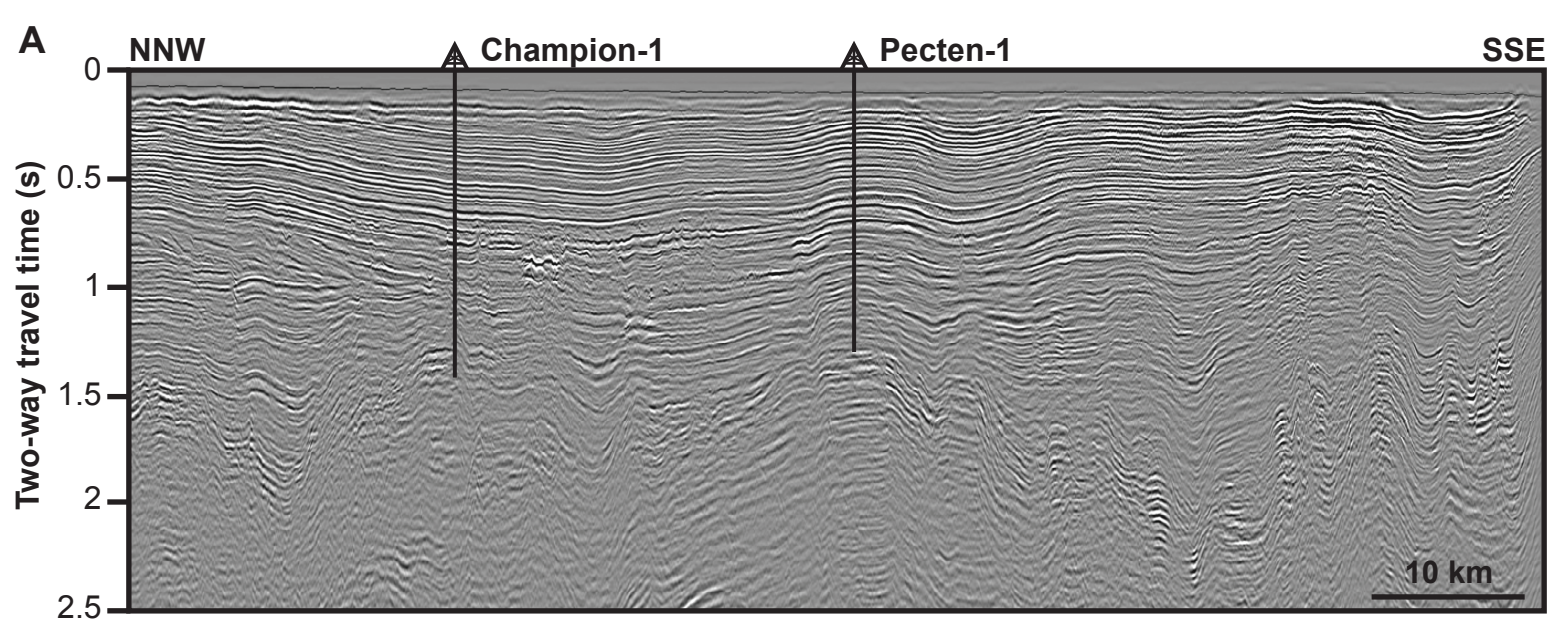


Holford et al Figure 8

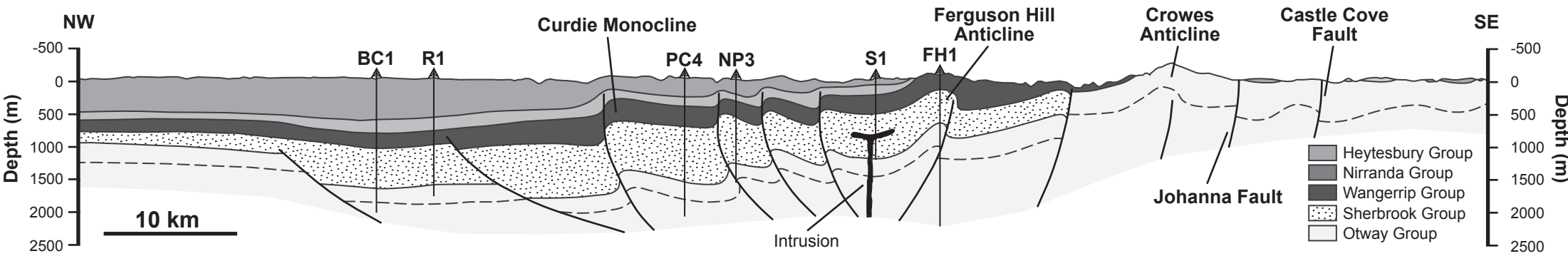


Holford et al Figure 9

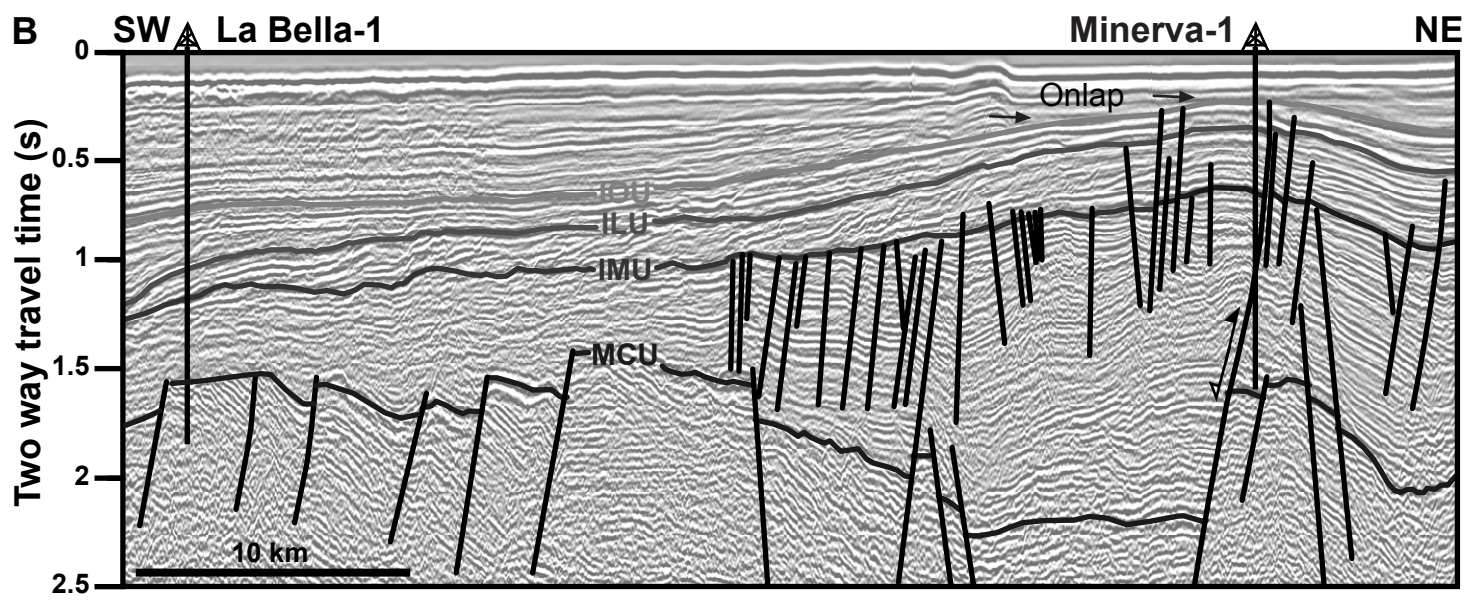
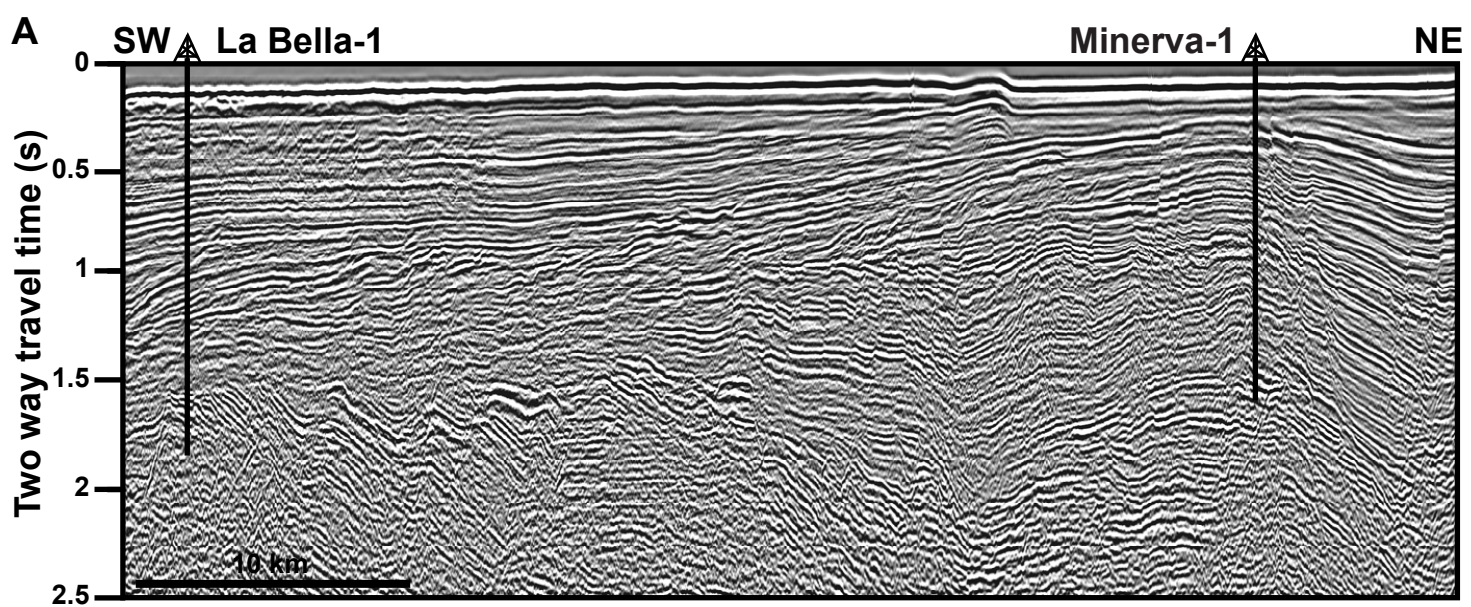




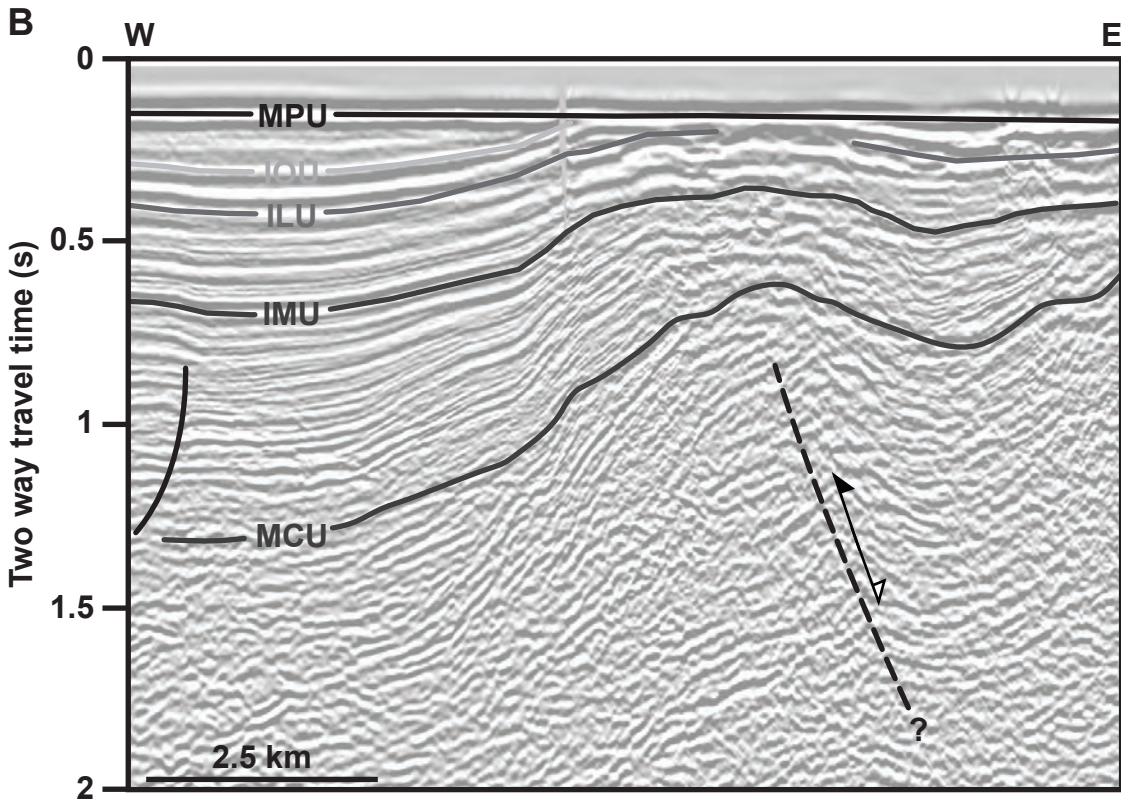
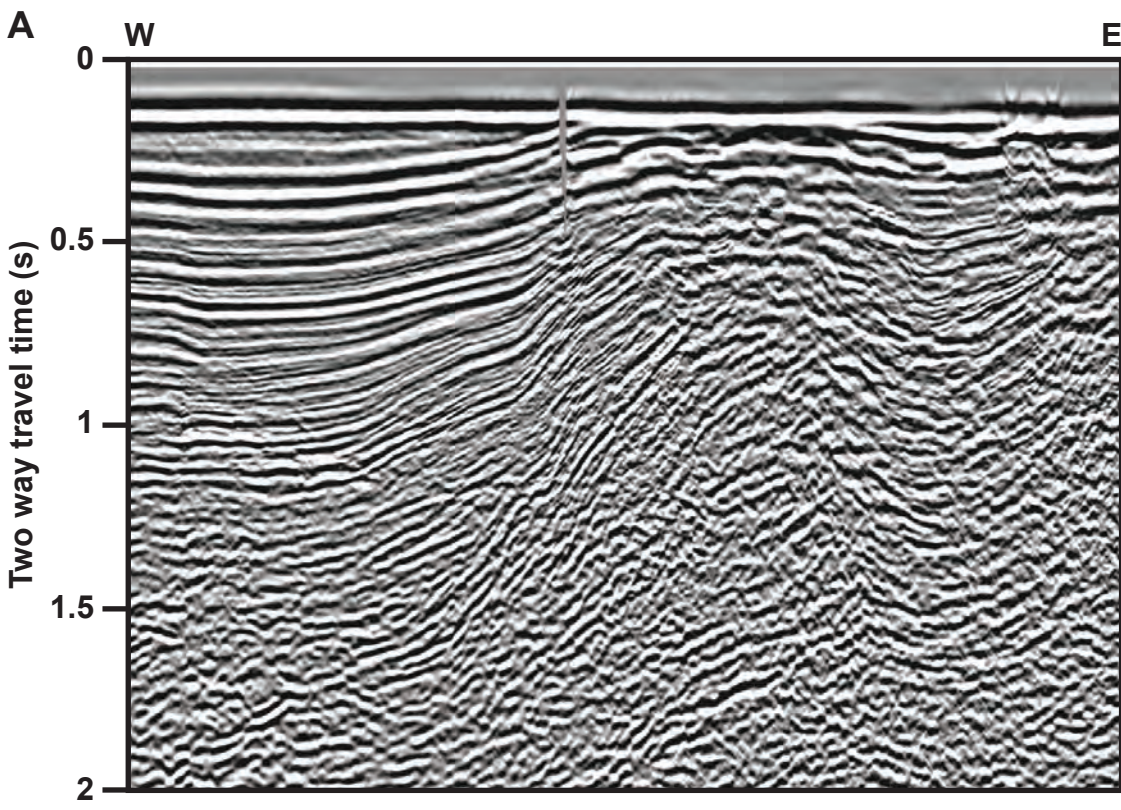
Holford et al Figure 11

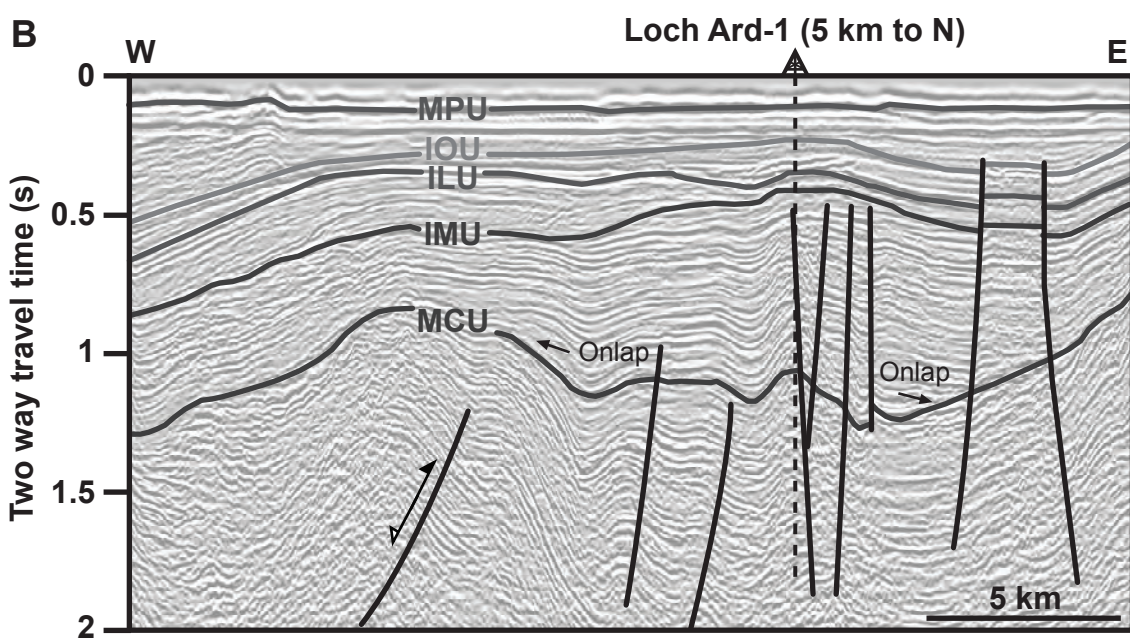
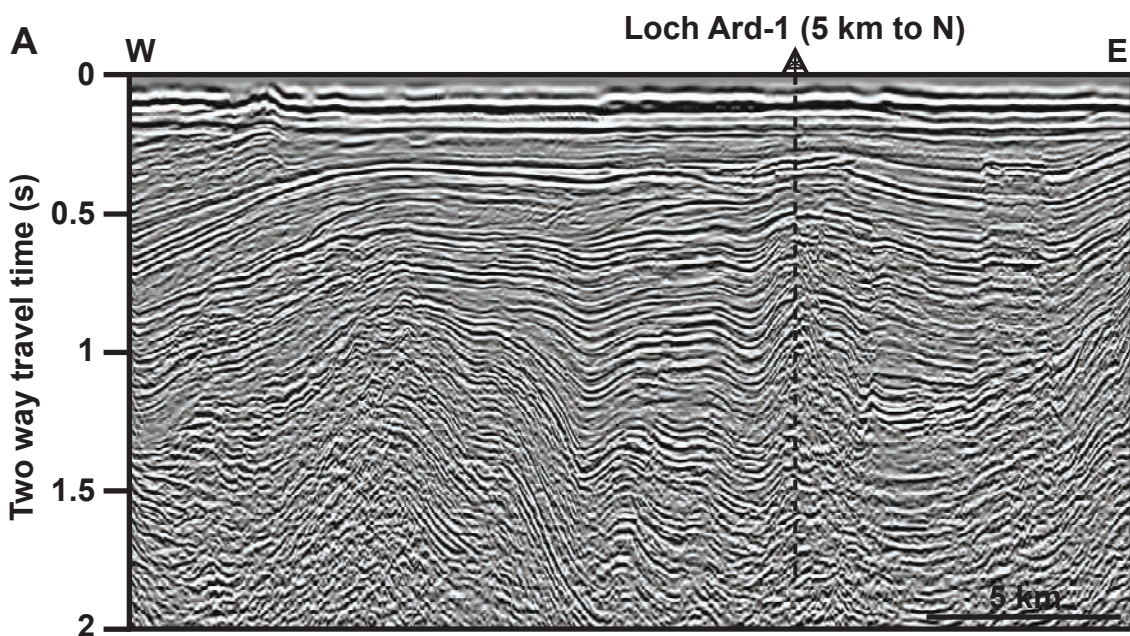


Holford et al Figure 12

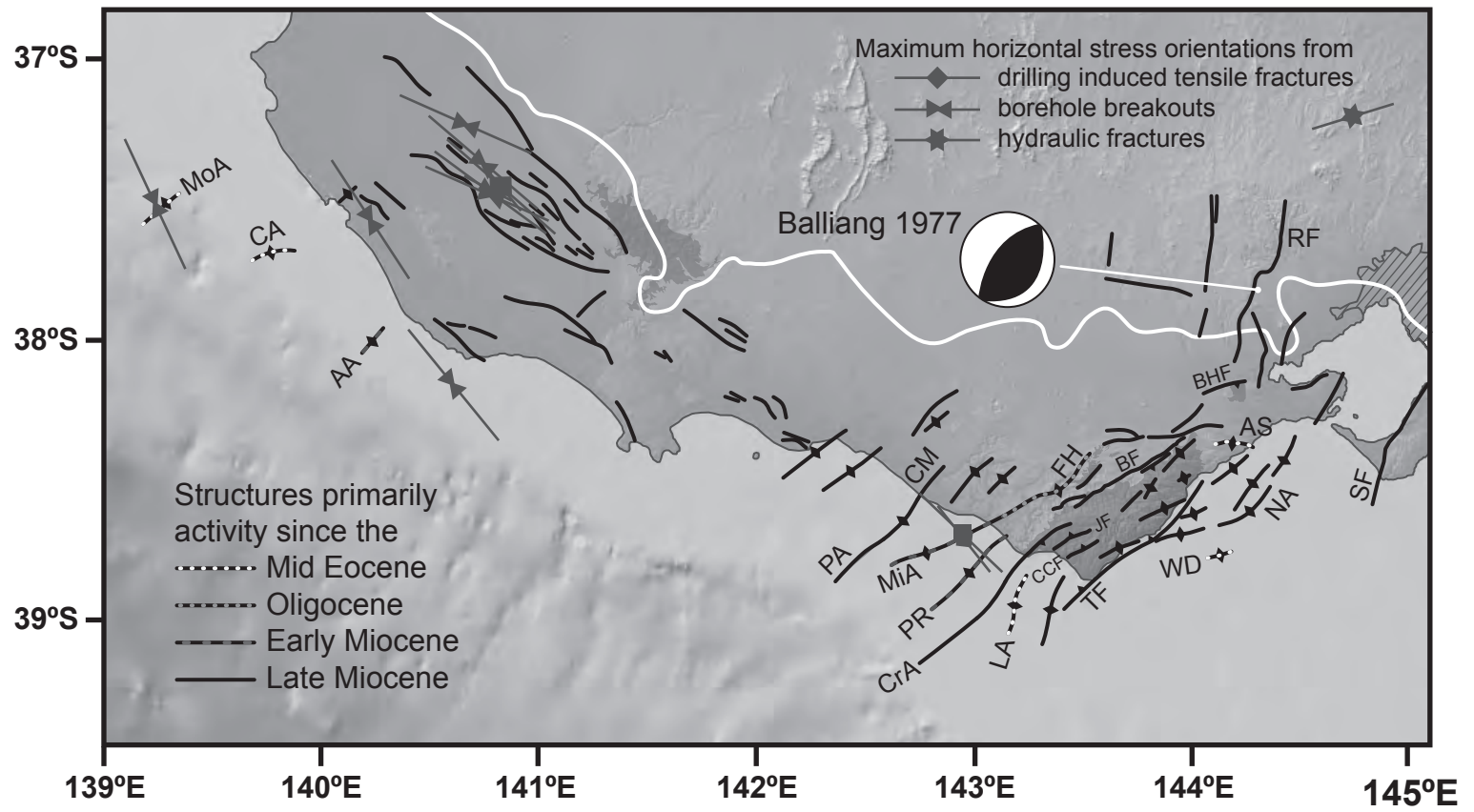


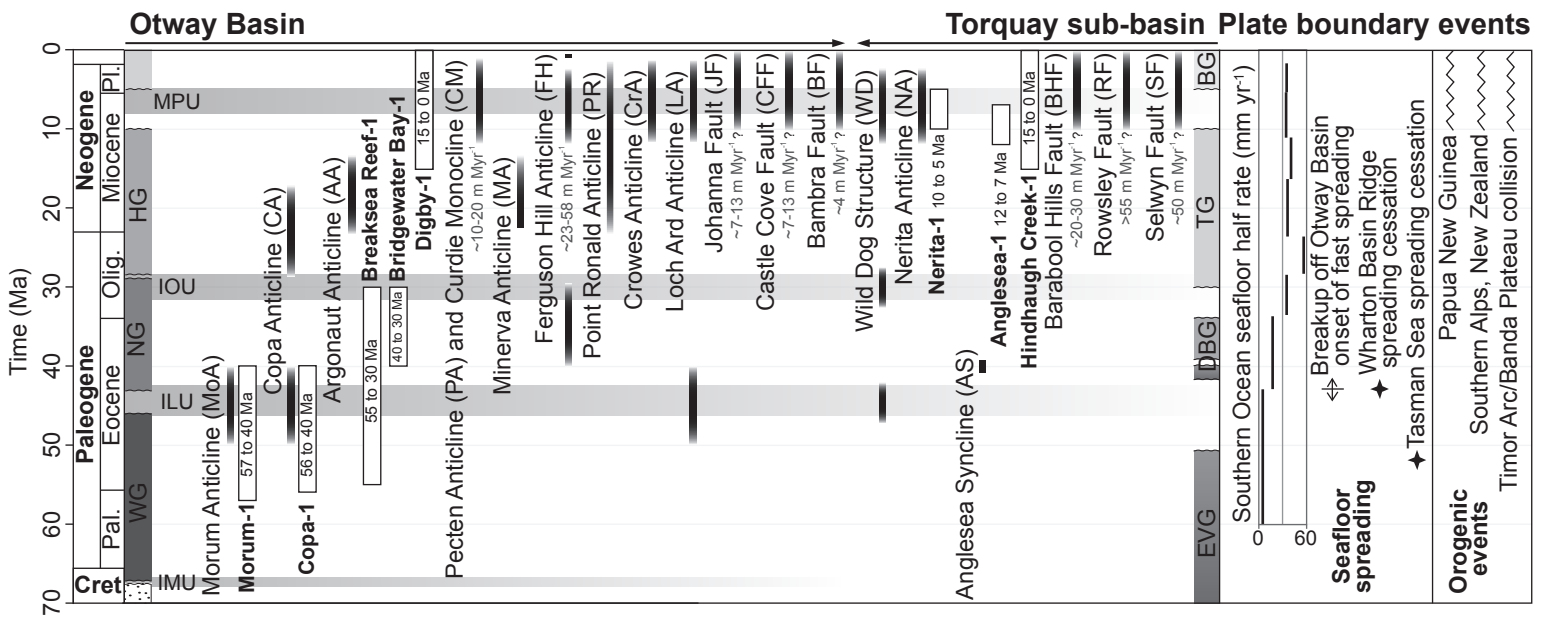
Holford et al Figure 13





Holford et al Figure 15





Holford et al Figure 17

